UiT The Arctic University of Norway

The Faculty of Bioscience, Fisheries and Economics
Department of Arctic and Marine Biology

Developmental effects of embryonic exposure to a water-soluble fraction of crude oil on early life stages of capelin (*Mallotus villosus*)

Adina Cassandra Granlund
Master's thesis in Biology (BIO-3950), May 2020

Frontpage: Capelin embryos at 25 days post fertilization. The photo is taken on the last day of crude oil exposure.

Table of Contents

List of figures

Abstract

The rise in offshore oil and gas operations, maritime shipping and tourism in northern latitudes enhance the risk of petroleum pollution and anthropogenic impacts of oil-related compounds on sub-Arctic and Arctic organisms. In particular, there is a need to investigate the potential adverse effects of petroleum to the early life stages of capelin (*Mallotus villosus*), an important forage and commercial fish species that spawn along the coast of Northern Norway. In this study, newly fertilized capelin embryos were exposed to five concentrations (control, low, medium, high and extra high) of a water-soluble fraction (WSF) of crude oil using oiled gravel columns loaded with either clean gravel (control) or gravel loaded with between 0.19 and 6 g oil/kg gravel (low to extra high groups). Embryos were exposed to decreasing crude oil WSF until hatch (25 days post fertilization) and larvae were followed in clean water until 58 days post fertilization. The initial aqueous total polycyclic aromatic hydrocarbon (PAHs) levels (sum of 44 PAHs) were ranging from 0.072 to 19.25 µg/L in the five treatment groups and decreased exponentially over time. None of the measured endpoints regarding embryo development and mortality, larval length, growth rate, cardiac activity, arrhythmia, and larval mortality showed any dose-dependent effects. Our results suggest that the early life stages of capelin are more robust to crude oil exposure than similar life stages of other fish species. The capelins demersal eggs properties, primarily the double-layered chorion, was hypothesized to be a possible explanation for this trend. To verify this hypothesis, further investigation of accumulated levels in embryos and how eggs morphology affects accumulation could be investigated.

Keywords: Crude oil, capelin, early life stages, oil spill, developmental toxicity.

Acknowledgements

The past year has been filled with a demanding but a rewarding academic journey, from struggling with statistical principles and coding in R to gaining knowledge about capelin and all its glory. The last semester has been surreal due to the coronavirus, with everyday life turned upside down, not being allowed on campus, and having digital lectures and examinations. Even though we made it through! I have learned so much on both an academic and personal level and I am incredibly thankful for all the people who helped me get there.

First and foremost I want to send a huge thank you to my one of a kind supervisor, Jasmine Nahrgang. Jasmine, thank you for the continuous help and the super quick replies to all my emails, even when the entire world was set on hold. For all your support and scientific advice. I am truly grateful for this opportunity and all the help you have given me.

Secondly, I would like to thank my lovely lab-partners Morgan Bender and Juliette Lavarec for the excellent mood and great cooperation during the long days we spent at Kraknes (counting and counting and counting larvae). Both of you made this experiment a pleasure to partake in. An extra thanks go to Morgan for teaching us the methods used in the lab, keeping us organized, and taking great notes. Marianne Frantzen and the entire Akvaplan-niva team at Kraknes, thank you for the opportunity to participate in this experiment, for the waffle-Fridays, kindness, help, and for feeding the larvae so I could celebrate the 17th of May in bunad.

Statistical advice from Michael Greenacre was greatly appreciated.

Lastly, I am forever grateful and thankful for the support of my incredible friends, family and boyfriend. Thank you for listening to my endless talks about my statistical problems and other capelin related issues during this period. For helping me through this surreal period in the world and keeping me motivated even though some days at the home office were rocky. Thank you for all the lovely moments I had with you, they were more than welcome breaks. For toppturer, hiking, and cross country skiing trips in all kinds of weather (and sometimes even sunshine), trying to teach me how to surf, lovely dinners, and video chats during the quarantine. Rinaldo, thank you for your patience and your marvelous R skills.

Abbreviations

°C	Degree Celsius
CEWAF	Chemically-enhanced water-accommodated fraction
Dpf	Days post fertilization
DWHOS	Deepwater Horizon oil spill
EC_{50}	Effect concentration of drug that gives half maximal response
ELS	Early life stages
EVOS	Exxon Valdez oil spill
GoM	Gulf of Mexico
L	Liter
LOD	Level of detection
LOEC	Lowest observed effect concentration
µg	Microgram
mL	Milliliter
mm	Millimeter
ng	Nanogram
PACs	Polycyclic aromatic compounds
PAHs	Polycyclic aromatic hydrocarbons
SEM	Standard error of the mean
UCM	Unresolved complex mixture
WAF	Water-accommodated fraction
WSF	Water-soluble fraction
Σ	Sum

1 Introduction

1.1 Oil spills and the need to investigate them

Oil is currently the dominant energy source in the world, and it is expected to remain so over the next several decades. The worldwide extraction, transportation, and use of petroleum inevitably result in its release to the environment (Wang et al. 2006). Crude oil is one of the most common pollutants released into the marine environment (National Research Council 2003). Over the past 40 years, oil extraction and transport have resulted in more than 340 major marine oil spills, primarily in coastal ecosystems, releasing over 3900 million metric tons of crude oil into the environment (Anderson et al. 2012). The dramatic ecological impacts of crude oil on marine ecosystems and fisheries has received much attention both in the past and in recent years. Particularly concerning major spill events such as the 1989 Exxon Valdez oil spill (EVOS) in Alaska, and the 2010 Deepwater Horizon oil spill (DWHOS) in the northern Gulf of Mexico (GoM) (Sørensen et al. 2017). The DWHOS event lasted for 87 days, and roughly 3.19 million barrels of oil were released into the ocean during the spill. More than 2100 km of shoreline was affected, including beaches, marshes, wetlands, and estuaries that are important habitats and nursery areas for a wide range of species (Beyer et al. 2016). Although catastrophic oil spills are not the most important source of crude oil discharge into the sea, they have strong acute and long-term impacts on marine ecosystems, including effects from physical damages and toxicity of their chemical compounds. Physical damages of crude oil include smothering, coating or fouling of oil on birds, mammals or other organisms (National Research Council 2003). Oiling of fur or feathers causes loss of insulation capacity, which can lead to hypothermia, smothering, drowning and ingestion of toxic crude oil (Peterson et al. 2003). Toxicological effects on species and habitats in the Gulf of Mexico have been documented in among other benthic and pelagic fish communities, zooplankton, mammals, birds and turtles (Almeda et al. 2014; McClain et al. 2019; Tarnecki and Patterson 2015). Effects from crude oil exposure can manifest at the population level as increased mortality or as sublethal impairment on the organisms' ability to forage, reproduce and avoid predators. Second-order effects, including trophic cascades, may take years to reveal themselves and to resolve (Peterson et al. 2003).

1.2 Crude oil composition and weathering

1.2.1 Composition

Crude oils consist of complex mixtures of hydrocarbons and non-hydrocarbons that range from small, volatile compounds to large, non-volatile ones (Wang et al. 2006). Crude oils can vary grossly depending on the geological source, and each type of oil has certain unique characteristics or properties which influence the oils' behavior, fate and effects in the environment (Fingas 2015; Wang et al. 2006). The major components of crude oil are hydrocarbons, such as paraffins, naphthenes and aromatics. Non-hydrocarbon constituents of crude oil include organic derivatives of nitrogen, oxygen, sulfur and metals (Speight 2014). Polycyclic aromatic hydrocarbons (PAHs) constitute 0.1-1% of most crude oils and are the most studied toxic components of crude oil. Chemically the PAHs are comprised of two or more benzene rings, with an increasing molecular weight with additional rings (Abdel-Shafy and Mansour 2016). PAHs are known to have high lipophilicity and persist long after the release into the environment (Bence et al. 1996; Cram et al. 2004; Yim et al. 2007). A lesser-known part of crude oil compounds is unidentified and commonly known as the unresolved complex mixture (UCM) (Farrington and Quinn 2015). The UCM from crude oil may have up to 250 000 compounds and makes up a larger fraction of the crude oil water-soluble fraction (WSF) than PAHs (Melbye et al. 2009; Sutton et al. 2005). Even though UCM-components are less studied than PAHs in WSF, a few studies show that a large fraction of this non-PAHs is bioavailable (Donkin et al. 2003; Melbye et al. 2009; Petersen et al. 2017). There are differences in the bioavailability of crude oil compounds, depending on whether the spilled oil is present as a surface slick, as dispersed oil droplets, or in dissolved form (Chakraborty et al. 2012; Jurelevicius et al. 2013). It is generally considered that the dissolved WSF of crude oil is the most bioavailable to marine organisms, and therefore contributes most to bioaccumulation (Hansen et al. 2018).

1.2.2 Weathering

After crude oil is spilled, several natural processes act together upon the oil to degrade it. These processes are referred to as oil weathering processes and significantly alter the crude oil properties, especially density and viscosity (Mishra and Kumar 2015). Weathering processes include spreading, evaporation, dispersion, emulsification, dissolution, biodegradation and chemical modification by oxidative processes (Faksness and Brandvik 2008; Wang et al. 2006). Abiotic factors like sunlight, temperature, wind and wave action have a significant

impact on the speed of those weathering processes (Faksness and Brandvik 2008). The extent of oil weathering differs substantially between spills and this, in turn, affects the chemical composition of the bioavailable fraction and resulting toxicity. In the Arctic, discharged oil will be more affected by other environmental conditions than in temperate regions, particularly lower temperatures, the possible presence of ice, and different light conditions (Brandvik and Faksness 2009; Faksness and Brandvik 2008).

1.3 Crude oil toxicity to early life stages of marine fishes

It is generally accepted that the early life stages (ELS) of fish are the most vulnerable to crude oil toxicity, due in part to their limited mobility, large surface to volume ratio, and lack of fully developed detoxification mechanisms (Mager et al. 2017). Embryos at the early stages of organogenesis have limited capacity for metabolism, leading to high bioconcentration of dissolved polycyclic aromatic compounds (PACs), which is readily detoxified and eliminated from larger (juvenile or adult) fish (Incardona 2017). Exposure to crude oil, even at very low concentrations, in developing fish is hypothesized to act through multiple pathways causing developmental toxicity and sublethal effects that may persist to later life stages (Carls et al. 1999; Hicken et al. 2011; Laurel et al. 2019; Mager et al. 2014). Due to their high sensitivity to pollution, ELS of fish, including embryo and larval stages, have been studied extensively (Sørensen et al. 2017). Different studies have reported that embryo exposure to WSF of crude oil can lead to both lethal and sublethal effects in a dose-dependent manner, particularly during early cleavage stages and during heart development (Beirão et al. 2019; Cherr et al. 2017; Incardona et al. 2011). Low levels of the water-soluble fraction can lead to significant developmental effects on fish embryos (Incardona et al. 2009).

The main sublethal, toxic responses in ELS of fish include cardiotoxicity and morphogenetic defects, as well as reduced size at hatch, which compromises later larval survival and could affect population recruitment (Frantzen et al. 2012; Incardona 2017; Incardona et al. 2015; Nahrgang et al. 2016). The discoveries of the mechanisms of toxicity for oil effects on ELS of fish arose from laboratory studies on developmental cardiotoxicity in response to the EVOS and is now one of the most frequently assessed endpoints associated with oil exposure (Incardona et al. 2013; Pasparakis et al. 2019). Numerous studies exploring the effects of crude oil on fish ELS have concluded that PAHs, and especially those from weathered WSFs and water-accommodated fractions (WAFs), were the components responsible for the

observed toxic responses (Carls et al. 1999; Heintz et al. 2000). Multiple studies have additionally indicated that 3-ringed (tricyclic) PAHs as the most damaging and cardiotoxic, in particular to the sensitive ELS of fish (Esbaugh et al. 2016; Incardona et al. 2014). This claim has recently been challenged by Meador and Nahrgang (2019). They find the lack of studies demonstrating that the sum of PAHs is capable of causing toxic effects in ELS fish at the low levels claimed (0.1−5 µg/L) (Carls et al. 1999; Cherr et al. 2017) without being part of a complex crude oil mixture noteworthy. Consequently, this causes the exclusion of the toxic potential of the non-PAH fraction. Therefore, they conclude that it is likely that numerous additional components in the WSF contribute to the toxic response (Meador and Nahrgang 2019).

Cardiotoxic effects at embryonic age following sublethal exposure to crude oil are shown to influence fitness and survival to adulthood. These effects include altered cardiac morphology and reduced aerobic capacity in adult zebrafish (Hicken et al. 2011), reduced swimming performance as adults after acute exposure as embryos in red drum (Johansen and Esbaugh 2017; Nelson et al. 2017; Stieglitz et al. 2016b) and reduction in adult survival for pink salmon (Heintz et al. 2000). The latter is shown by a series of mark and recapture studies with an average reduction in adult survival by 36% (Heintz 2007; Heintz et al. 2000). In addition, there is evidence of strong population effects for pink salmon, for which studies of embryos in spawning gravel in the intertidal zone of streams crossing oiled beaches demonstrated elevated mortality for at least four years after the EVOS (Rice et al. 2001). Findings that transient embryonic oil exposure affects the performance of several species of adult fish, in addition to the documented population-scale effects of pink salmon exposed to EVOS oil during ELS, strongly suggest a link between individual-based toxicity and population-level response (Hicken et al. 2011). Furthermore, the survivors of these exposures can display sublethal effects that ultimately interact with other environmental stressors, further reducing the survival of the exposed population (Heintz et al. 2000).

1.4 Capelin (*Mallotus villosus*)

Capelin (*Mallotus villosus*) is a subarctic species that has a circumpolar, primarily sub-Arctic distribution throughout regions of the Pacific and Atlantic Oceans (Hop and Gjøsæter 2013; Rose 2005). Capelin has long been recognized as an essential forage and commercial fish species in the Northwest Atlantic ecosystem. The capelin stock is the largest stock of pelagic

fish in the Barents Sea and plays a vital role in the arctic food web due to possibly having the largest stock size in the world (Gjøsæter 1998). Capelin carries energy from the northern to the southern regions in the Barents Sea during its extensive migrations (Hop and Gjøsæter 2013). Through its function as a forage fish, capelin funnels energy to higher trophic levels such as other fish species, marine mammals, and seabirds and produces annually more biomass that the weight of the standing stock (Gjøsæter 1998). During the last four decades, the capelin stock in the Barents Sea has undergone several collapses in stock size. The drastic reduction in capelin biomass led to detrimental effects on predators such as the economically important cod, sea birds and mammals in various ways (Gjøsæter et al. 2009; Tairova et al. 2019).

Capelin is a small and short-lived pelagic species, with a maximum life span of 7 years in cold waters (Vilhjálmsson 1994). Males grow to a maximum length of ca. 20 cm and females 18 cm, their weight seldom exceeds 50 grams (Gjøsæter 1998). The growth has been found to vary with stock size, water temperature and geographical distribution (Gjøsæter and Gjøsæter 1986). Due to the short lifespan of capelin, the stock size is strongly dependent on recruitment. Capelin may undertake extensive spawning and feeding migrations (Gjøsæter 1998; Vilhjálmsson 2002), or spend most of their lives within a limited geographical area as the inshore capelin (e.g., from Norwegian fjords) does (Brown 2002). In general, capelin matures at 3 to 5 years of age. Capelin spawn on beaches in the intertidal zone or offshore in deeper oceanic waters, and the spawning habitats employed by capelin populations differ markedly with zoogeography (Christiansen et al. 2008). The spawning foregoes on a substrate (coarse sand), and capelin displays one of two different modes of reproductive behavior. They are typically semelparous (i.e., spawn once and die) or iteroparous (two or more spawning events before death). The latter is known to occur for the beach-spawning capelin (Christiansen et al. 2008; McNicholl et al. 2018). Capelin spawns 1 mm demersal eggs during spring and summer in waters outside northern Norway and northwestern Russian (Murman) coast (Gjøsæter 1998; Gjøsæter and Gjøsæter 1986; Hop and Gjøsæter 2013).

The beach-spawning capelins eggs are exposed to vast and regular fluctuations in temperature and salinity during diurnal tidal periods, mechanical actions from waves, sunny weather, and droughts. Capelin eggs are shown to be quite resistant to various environmental fluctuations and display no significant mortality after being exposed to prolonged periods of sub-zero temperatures (Præbel et al. 2009). The capelin eggs have a thick and more complex chorion,

which is more resistant to mechanical damage, similar to herring and sculpins, among others. The eggs of the Balsfjord capelin are shown to survive in a super-cooled state due to the double chorion that prevents penetration of ice crystals from the environment (Davenport and Stene 1986). Besides, demersal eggs have a large amount of yolk and a period of development for up to two months, in contrast to pelagic eggs which generally have a thin chorion, a small amount of homogeneous yolk, and develop typically within a week (Lønning et al. 1988; Miller and Kendall Jr. 2009). Depending on the temperature, capelin hatch after ca. 34 days (Gjøsæter and Gjøsæter 1986). Post-hatch, the larvae drift using ocean and wind-induced surface currents (Gjøsæter 1998). After the larval stage, the immature ocean capelin often migrates long distances to find suitable feeding grounds, whereas inshore capelin in local populations might complete their entire life cycle without migrating out of fjords and nearshore waters (Brown 2002; Vilhjálmsson 2002). The Barents Sea capelin undertakes spawning migrations across vast geographical distances (Behrens et al. 2006).

1.4.1 Capelin and anthropogenic activities

How petroleum products affect this keystone species is not well understood, despite current and substantial oil extraction and activities occurring nearby critical spawning habitats (Beirão et al. 2019). Capelin serves essential functions in the marine ecosystem, and changes in their abundance, distribution and competition for food resources will have consequences for the energy flow in marine food webs leading up to predatory fishes, marine mammals and seabirds (Hop and Gjøsæter 2013). A wide range of shipping activities takes place throughout the Barents Sea, involving among other shipping vessels and cruise ships (Novikov et al. 2011). As Northern waters become increasingly accessible as a result of a warming climate, offshore oil and gas operations, maritime shipping and tourism are all expected to increase over the coming years (Rossi 2013). Ship traffic in the Arctic region has increased by 60% since 2012 (Champine et al. 2019), especially in the Barents Sea and along the Northern Sea Route, which traverses feeding-, wintering- and spawning areas for capelin in the Barents sea (Eguíluz et al. 2016; Gjøsæter et al. 2011; Huse and Ellingsen 2008; Smith and Stephenson 2013). The rise these activities leads to a growing focus on the potential effects of oil pollution on Arctic marine ecosystems due to the increased risk of petroleum pollution in Barents Sea ecosystem (Novikov et al. 2011). Furthermore, this could be particularly problematic if overlapping in space and time with capelin reproduction (Beirão et al. 2019).

Recruitment could be significantly impacted if an oil spill with environmentally realistic concentrations occurred in the vicinity of capelins spawning grounds (Beirão et al. 2019; Frantzen et al. 2012; Paine and Leggett 1992; Tairova et al. 2019). Capelin form dense schools in nearshore areas and spawn during a short reproductive season. Within that period, capelin are particularly susceptible to the effects of oil spills that could concentrate nearshore (Penton and Davoren 2013). In general, there is a lack of validated toxicity data for most Arctic species. Thus, there is an urgent need to acquire further experimental data on the effects of spilled crude oil on ELS of cold-water marine fish, regarding bioaccumulation, critical body burden and how dispersed crude oil droplets affect fish ELS (Olsen et al. 2013; Tairova et al. 2019). In regards to capelin, there is a call for more experiments investigating the sensitivity to crude oil at specific developmental time points, surrounding critical periods of development and morphogenesis.

1.5 Aim of the study

Major oil spills like the EVOS in 1989 and the DWHOS in 2010 have led to many studies investigating the adverse effects of crude oil exposure on marine fishes and their early life stages (Heintz et al. 2000; Incardona et al. 2014; Incardona et al. 2013; Mager et al. 2014). The objectives of this study are to elucidate the biological effect of ELS capelin to crude oil WSF. For that purpose, to mimic field conditions after a major oil spill, exposure of capelin eggs aggregated in gravel was done using oiled gravel columns to deliver WSF of crude oil into the water (Carls et al. 1999). Building on acquired knowledge (Frantzen et al. 2012; Nahrgang et al. 2016; Bender et al. in preparation), the project focuses on embryo- and larval mortality and sublethal effects including development, growth, and cardiac activity. Based on previous studies, we hypothesized that early life stages of capelin would show a dose-dependent decrease in growth, impaired cardiac activity, and an increase in mortality for the higher exposure doses.

Additionally, uptake and excretion of hydrophobic compounds is depending on the ability of these chemical to path across the chorion of fish eggs (Brinkworth et al. 2003). The chorion is thus playing a role in the rate of exposure and response of fish embryos to crude oil WSF exposure. The chorion of pelagic eggs is thinner than that of demersal eggs (Miller and Kendall Jr. 2009). Therefore, given the thicker chorion of demersal capelin eggs, we

hypothesized that capelin eggs would show lower sensitivity to crude oil WSF exposure compared to similar studies on pelagic eggs.

2 Material and methods

2.1 Ethical statement

The present experimental work was done according to regulations enforced by the governmental Norwegian Animal Research Authority (ID 19371). The author has appropriate training (equivalent to FELASA C) to perform the work.

2.2 Collection of the capelin eggs

On the 13th of April, beached-spawned capelin eggs deposited on coarse sand were collected at 11 a.m in Loddebukta, Balsfjorden (N 69°14', E19°13'). The eggs were kept cold and humid until arrival at Akvaplan-niva's research station at Kraknes. Upon arrival, the egg-bearing coarse sand was placed in a clean flow-through water tank (5°C, filtered 60 µm and UV-treated seawater) until the start of the experiment the next day. Embryos were studied under a stereomicroscope and estimated to be 6 days post fertilization (dpf) at the beginning of the experiment, corresponding with the crack of optic bulb developmental stage, just before the end of organogenesis 1 (Fridgeirsson 1976).

2.3 Experimental design

The experiment used five oiled gravel PVC columns designed for studies on embryotoxicity by Carls et al. (1999) following the Exxon Valdez oil spill. The goal of this experiment was to simulate an oil spill on beach gravel and the following exposure of capelin embryos to the water-soluble fraction of crude oil. The experimental design used mimics the continuous weathering of crude oil, which leads to an exponential decrease in oil concentration and change in the WSF oil compositions over time. Therefore, four treatment groups (low, medium, high and extra high) with different concentrations of crude oil and a control group were set up. Each of the five groups was replicated four times, which generated a total of 20 experimental incubators.

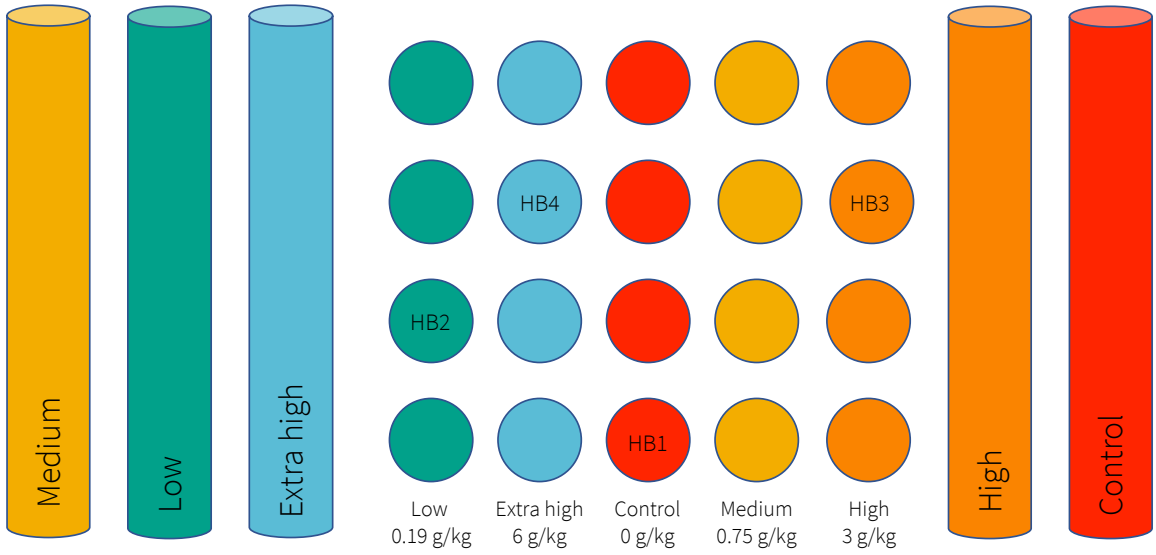

Figure 1: Incubator setup for the exposure of crude oil (T0 – T19). Five treatments and four replicates per treatment group. Crude oil concentration each treatment group received per kilo of gravel (0 g/kg, 0.19 g/kg, 0.75 g/kg, 3 g/kg and 6 g/kg) is marked under each column. Exposure lasted from the first day of the experiment (T0), until day 19 (T19). HB(1-4) marks random incubators containing HOBO® logger (Onset®) to record light and temperature every four hours.

The oiled gravel columns were prepared according to (Carls et al. 1999; Incardona et al. 2015; Nahrgang et al. 2016) with slight modifications. Briefly, gravel (7-9 mm) were washed with freshwater, soaked in 1M HCl for at least one hour, rinsed, and left in 90% ethanol overnight. The following day the gravel was rinsed again before it was dried at 60°C for 10-12 hours. The gravel was then coated with crude oil (Kobbe oil from the Barents Sea Shelf) at four different concentrations: low (0.19 g/kg), medium (0.75 g/kg), high (3 g/kg) and extra high (6 g/kg). The control was washed in the same way, but not coated with crude oil. After the coating, the gravel were air-dried for three days at ambient temperature (7°C). The gravel destined for the control treatment was kept separately during drying to avoid cross-contamination. Then, 1 meter high PVC columns were loaded with 11 kg of oiled gravel (or clean control gravel), repeated for all treatments (n=5). The columns were capped with aquarium filter floss to prevent oil droplets from entering the effluent water. In total, five columns (5 treatments) got connected to replicate incubators and flushed for 70 hours with filtered (60 µm) and UV-treated seawater at a flow rate of 22.5 L/h. The flushing aimed to remove the highly volatile and acutely toxic BTEX (benzene, toluene, ethylbenzene, and xylene) compounds before exposure start. The columns were prepared in advance of the experiment and were frozen at -20°C after initial flushing.

2.3.1 Exposure of capelin embryos to crude oil water-soluble fraction (WSF)

Egg density per gram of substrate (coarse sand) was determined by weighing and counting four sub-samples (30.8 g) of the substrate to achieve a similar embryo density in each incubator. The capelin eggs were distributed into twenty experimental incubators of six liters at a density of n = 8095 ± 1047 eggs per incubator. The water flow was connected to the oiled gravel columns and attached to the bottom of each incubator in the treatment groups. The incubators were kept in a flow-through system receiving filtered (60 µm) and UV-treated seawater, with a flow of 22.5 L/h per incubator. The entire egg-bearing substrate layer was elevated from the bottom of the incubator with a fine mesh netting to allow equal exposure of crude oil and better gas exchange within the incubator (Figure 3).

The temperature and 24h light regime were set up to correspond to the natural conditions of the capelin embryos to minimize the difference between the experimental and natural environment. Four HOBO® loggers (Onset®) were placed in one random incubator per treatment group except for the medium treatment (Figure 1). The loggers recorded light exposure and water temperature every four hours to vertify that the light exposure (17.7 ± 1.28 Lux during daytime) and water temperature (5.5 ± 0.26°C) were stable across treatments during the exposure.

2.3.2 Post-exposure experimental design

After 19 days of exposure (25 dpf), each of the twenty incubators (6L) containing egg-bearing substrate were inserted in 25L tanks to give the hatched larvae enough space to swim and grow (Figure 3). The 25L tanks were kept under similar conditions as the previous exposure incubators in terms of water temperature (5.3 ± 0.05 °C) and light (55.7 ± 3.27 Lux during daytime) until the end of the experiment (58 dpf).

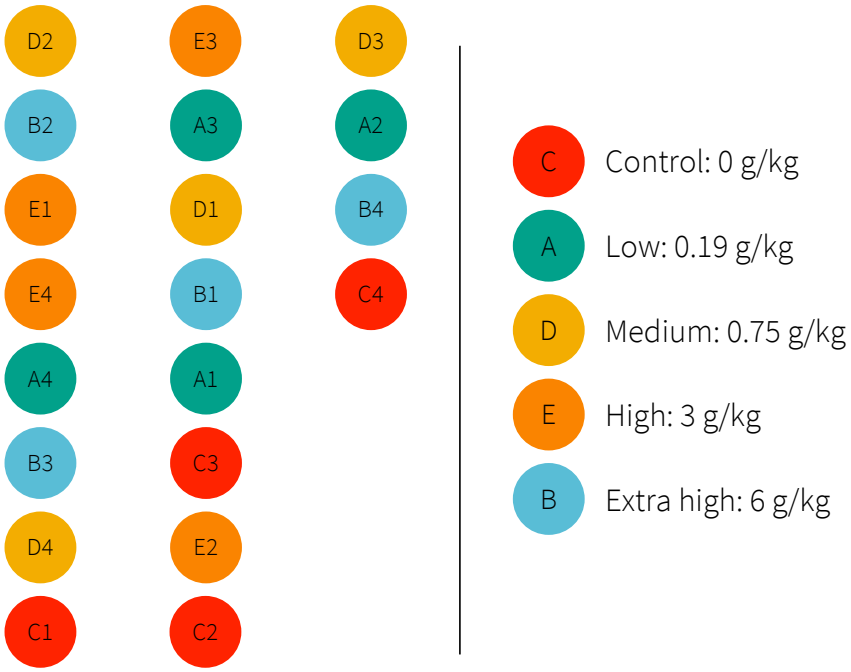

Figure 2: Randomized incubator setup post-exposure (T19 – T52) in 25L incubators. Each treatment group (A, B, C, D and E) and replicate (1, 2, 3 and 4) was named accordingly to ensure randomization and repeatability of the experiment. The unit g/kg represents each treatments concentration of crude oil in grams per kilo gravel.

The exposure was stopped at the transfer of the 6L incubators. From thereon, the capelin larvae only received uncontaminated filtered seawater (60µm, UV-treated, 25L/h). The 25L tank was set up with air stones for aeration, and the seawater outflow was covered in fine mesh to ensure that the larvae did not get flushed out. The aeration system was set in place to ensure that the larvae and the rotifer cultures used to feed the larvae did not adhere to the water surface, but mixed throughout the water column.

The first observed hatching was at 28 dpf. Hatching was further stimulated at 31 dpf by gentle shaking of the 6L incubators to assist larvae possibly stuck in the gravel to pass over to the larger tanks. End of hatching was marked at 36 dpf, when no more hatching was observed and the 6L incubators were removed from the 25L tanks. After that, the larvae were kept in the 25L tanks from where all further sampling was executed until the end of the experiment at 58 dpf.

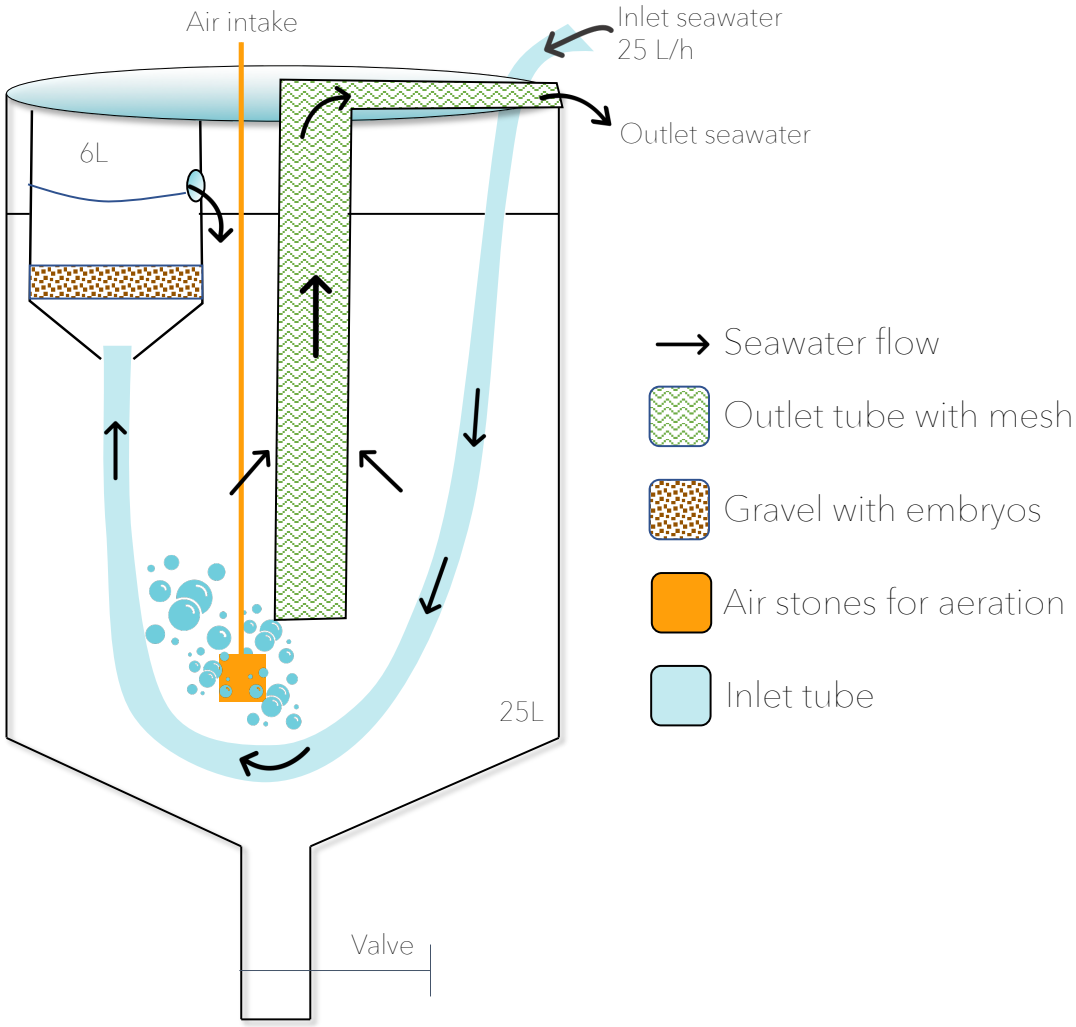

Figure 3: Post-exposure experimental setup for all 20 incubators from the end of exposure 25 dpf until 36 dpf. The flow of seawater is shown by arrows, leading the water flow through the bottom of the 6L incubator and out of a hole on the side. This allowed the larvae to swim into the 25L tank. The valve on the bottom was used for cleaning and sampling purposes.

2.3.3 Larvae feeding regime

Feeding of larvae was initiated at 30 dpf, soon after the beginning of hatching in collaboration with NOFIMA AS, who produced the rotifer cultures to feed the larvae. The live rotifers were mixed with green algae, *Nannochloropsis* (Nanno 3600, Reed Mariculture) to create a contrast for the food in the water column and thereby increase larval feeding success (Stuart and Drawbridge 2011). The larvae were fed three or four times a day with 250ml of live rotifers and algae mixture, representing 3-5 rotifers per ml per incubator until 51 dpf. Starting from 52 dpf (T46), the larvae were fed frozen rotifera since NOFIMA ended their rotifera production. Rotifera leftovers had been frozen into ice cubes at a concentration that would yield 3-5 rotifers per ml per incubator.

2.4 Timeline for the experiment

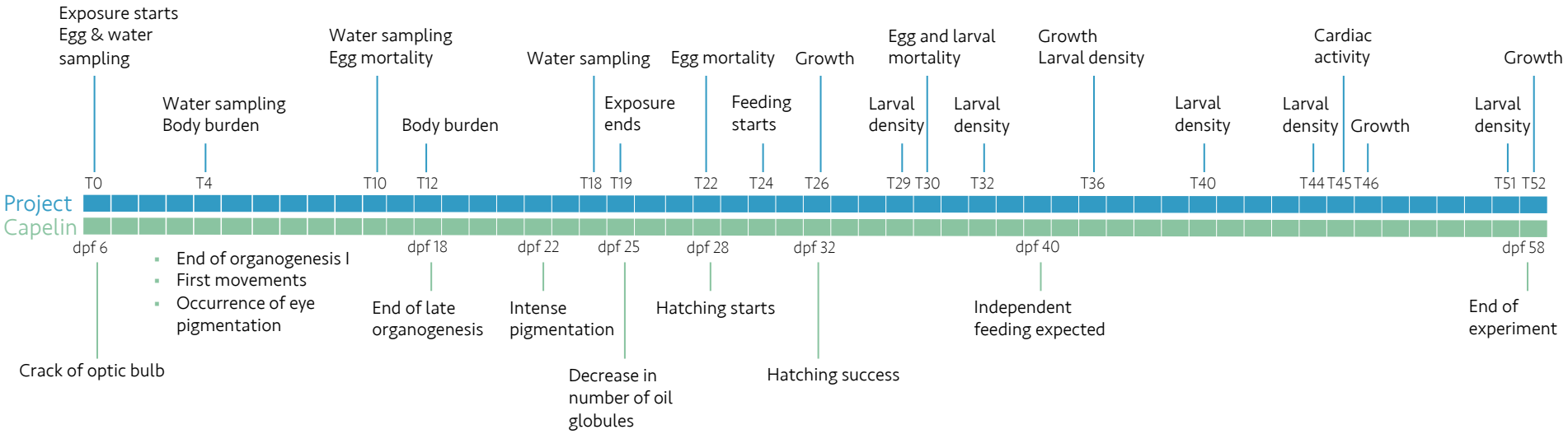

Figure 4: Timeline of the ELS capelin exposure to WSF of crude oil experiment. Project samplings and day (T) is represented by the blue line on the upper part of the figure. Capelin development based on dpf (days post fertilization) is shown on the bottom part of the figure presented in green. The first day of experiment T0 equals to 6 dpf.

2.5 Sampling and data analysis

2.5.1 Chemistry sampling and analysis

Water samples (1L in duplicates, per treatment column) were taken directly from the oiled gravel columns outlet at the start of the exposure (6 dpf), at 10 dpf, 16 dpf and 24 dpf to determine the chemical composition and levels of 44 PAHs in the WSF (n=40 total samples). The samples were stored in amber glass bottles at -20°C until the 1st of November 2019. Then 5 mL 15% HCl was added and the bottles placed in a fridge to thaw until shipping to SINTEF on the 4th of November. Upon arrival at SINTEF, the acidified samples were stored dark and cool (4 °C) until extraction. One sample per treatment and time point was analyzed for 44 PAHs by an Agilent 7890 gas chromatograph coupled with an Agilent 7010B triple quadrupole mass spectrometer fitted with an EI source and collision cell (Agilent Technologies, Santa Clara, CA, USA). The determination of PAH compounds was done according to previous studies by Sørensen et al. (2016). PAH concentrations below the level of detection (LOD) were set to zero.

2.5.2 Embryo and larval development and mortality

Sampling for estimation of the proportion of abnormal development and mortality was done on embryos during the exposure period (6 dpf until 25 dpf) at 16 dpf and right after hatching started at 28 dpf. For that, one subsample of egg-bearing substrate was taken from each incubator with a small spoon and distributed in a Bogorov counting chamber. The embryos were observed under a Leica M205 C stereomicroscope with a camera (Leica, MC 170 HD), which was used for all samplings during the experiment. The embryos (min. n=50 per incubator) were classified in one of three categories: normal embryo, abnormal embryo development (i.e., black and not golden colored eyes, numerous oil globules in the yolk sac, smaller than normal body), and dead embryo. The eggs used for the sampling were not put back into the incubators.

Regarding larval mortality, direct mortality counts were not possible to conduct in this experiment. The sampling of sinking dead larvae individuals using the valve at the bottom of the 25L tanks did not allow us to exclude freely swimming larvae, thereby contaminating these mortality samples. Therefore, larval mortality was estimated through measuring changes in larval densities in the 25L tanks between 35 dpf, 38 dpf, 42 dpf, 50 dpf, and 57 dpf. Before sampling, the aeration strength was increased to homogenize the larval distribution and

optimize sampling precision. Briefly, three subsamples of 100 mL were collected from the well-homogenized water column of each tank, using a plastic tube (150 mL) that sampled water from the entire water column height of the 25L tank. The plastic tube was washed between each treatment to avoid contamination. Total density (larvae per liter) was estimated based on the total count in the sub-samples, and the decrease in density over time for each incubator was used as an indirect measure of mortality. Average larval densities (larvae per liter) of the triplicate sampling was calculated for each incubator at all sampling time points. All calculations were done using Microsoft Excel (Version 16.32).

2.5.3 Larval length and growth analysis

Larvae length measurements were taken every tenth day at 32 dpf, 42 dpf, 52 dpf, and one sampling at the last day of the experiment (58 dpf) to assess larval growth in millimeters. Briefly, aeration in the tanks were lowered and 30 larvae were sampled from the incubator surface. To reduce larval condition as a confounding factor, only larvae that were seemingly in good condition by visual assessment (i.e., swimming actively and normally pigmented) were picked from the 25L tank using a plastic pipette. The larvae (n=30 per incubator) were placed onto watch glasses (n=5 per glass) containing a drop of carbonated water to anesthetize the larvae during the procedure. All larvae were ordered in line to facilitate the measurements and data analyses.

Figure 5: Length measurement of a capelin larvae from incubator A2 (low treatment) at 52 dpf. All measurements were conducted from the heads center to the end of the tail, based on the 2mm scale shown in the picture.

All pictures were analyzed using the opensource software ImageJ (1.52q) to measure the larvae length in millimeters (to the nearest 0.001 mm). The specific growth rate (SGR) per incubator was calculated according to the following equation using records of initial (i) and final (f) total length (TL), based on incubator averaged length measurements (Nahrgang et al. 2019).

$$Eq.1: SGR\ (\%\ per\ d) = \frac{(lnTL_f - lnTL_i)}{Time\ in\ days} x\ 100$$

2.5.4 Imaging of heart and determination of cardiac activity

When the larvae were seven weeks into development, video recordings for heart rate (beats per minute) and arrhythmia analyses were conducted at 51 dpf. A temperature-controlled microscope stage was used to ensure that the larvae were kept at a constant cold temperature (5ºC) during the recording to minimize the potential effect of temperature stress on the heart. The larvae (n=5 at the time) that were seemingly in good condition (see section 2.5.3 for methodology) were picked from the 25L tank using a pipette. After that, the larvae were allowed to acclimatize on a cooling stage in a watch glass containing methylcellulose (3% in seawater) for a few minutes before the recording started. In total, twenty larvae from each treatment (n=100) were sampled and recorded for at least 1 minute.

For the cardiac recordings, a Leica M205 C stereomicroscope with a Leica MC 170 HD camera connected to Leica Application Suite was used. The larvae were kept stable and immobile during the filming process by the methylcellulose (3% in seawater). Photographs of the heart and body of the larvae after the recordings were taken to visually analyze potential malformation (i.e., craniofacial deformities and body axis defects). The intension of this analysis was to investigate if the larvae used in the sampling showed any correlation between the potential secondary effect of a reduction in cardiac function and cardiac activity measured. As no larvae showed any signs of malformation, data was not presented. Heart rate and cardiac arrhythmia were determined, according to Incardona et al. (2009). Briefly, the heart rate (beats per minute, BPM) was determined from counting heartbeats in 30-second video segments. Cardiac arrhythmia was assessed by determining the interbeat variability from the same video segments by counting the number of frames between the initiation of each cardiac contraction. The number of frames between heartbeats would be the same for regular heart rhythm and lead to a low standard deviation (SD) (i.e., <1), whereas a higher SD (i.e., >1), is a measure of an irregular heart rate (Incardona et al. 2009). The videos were all analyzed by

the use of VLC media player (Version 3.0.8 Vetinari). Using Microsoft Excel, the number of frames between heartbeat initiations was calculated, and the mean and SD obtained for each embryo (n = 20 per treatment).

2.5.5 Statistical analysis

All experimental data were analyzed with R version 3.6.3 and R Studio 1.1.463 and unless stated otherwise, all graphs are generated with the R package "ggplot2" (Wickham 2016). Normal distribution of residuals was assessed using a Shapiro-Wilk test, visual assessment of the Q-Q plot supported the test. If normality requirements were met (arrhythmia and growth rate), a one-way analysis of variance (ANOVA) with a subsequent Tukey HSD post hoc test on differences between means followed. If normality requirements were not met (cardiac activity in BPM), a Kruskal Wallis test, followed by a post hoc Dunn test was performed with Hommel corrections of the p-values. The threshold for statistical significance level was set to alpha = 0.05. Density and length measurements were log-transformed, for density 0.1 replaced 0 to avoid issues with log-transformation. A linear mixed effect model using the 'nlme' package (Pinheiro et al. 2020) evaluated the length and density data with treatment and time as fixed factors and incubators as a random factor, followed by an estimated marginal means (EMMs), (also known as least-squares means) with Tukey correction of p-values as a post hoc multiple comparison model. Fisher's exact test of independence with simulated p-value (based on 2000 replicates) was used to determine significant differences between treatments regarding embryo counts for normal, dead or abnormal embryos. When significant, the Fisher test was followed by pairwise comparison with False Discovery Rate (FDR) corrections of the p-values. All data in this thesis is presented as mean value with the standard error of the mean (SEM), unless stated otherwise.

3 Results

3.1 Water chemistry analysis

Water samples from the crude oil experiment taken at day 0, 4, 10, and 18 were analyzed for total sum (Σ) 44 PAHs, calculated from 44 parent and alkylated PAHs (Figure 6). The analysis of Σ44 PAHs showed that the waterborne exposure of capelin larvae was successful and dose-dependent. Initial Σ44 PAH concentration in the water were 19.25 µg/L, 9.36 µg/L, 1.95 µg/L, 0.53 µg/L, and 0.072 µg/L for treatments extra high, high, medium, low and control, respectively. The highest concentration was measured at day 0 (dpf 6), and Σ44 PAH declined over the experimental period for all treatments. For the last water sample taken at T18, the Σ44 PAH for treatment high almost doubled from T10 (dpf 16) and surpassed the extra high treatments final concentration. The potential reason for this might be a contaminated sample.

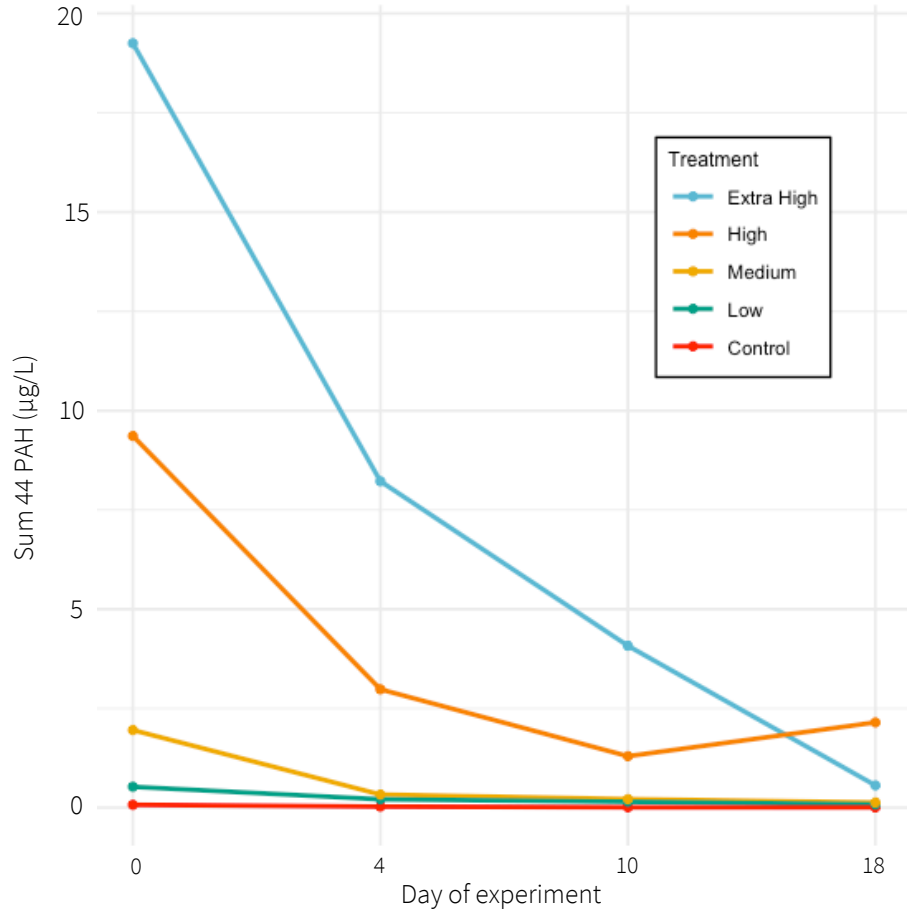

Figure 6: The total sum of 44 PAH concentrations (µg/L) in water by treatments as a function of time. Samples were taken at day of experiment T0 (6 dpf), T4 (10 dpf), T10 (16 dpf) and T18 (24 dpf). Day 0 represents the start of embryo exposure. Each point represents a single measurement. Different concentrations of crude oil are distinguished by color. Control: 0 g crude oil/kg gravel, Low: 0.19 g crude oil/kg gravel, Medium: 0.75 g crude oil/kg gravel, High: 3 g crude oil/kg gravel and Extra High: 6 g crude oil/kg gravel.

The relative abundance of the 44 PAH compounds analyzed in the WSF of crude oil changed throughout the exposure period (Figure 7). The predominant PAHs initially present at the start of the experiment (T0) where the smaller and less substituted PAHs, e.g., naphthalene and its alkylated homologs amounted for 79.9% of the total dissolved Σ44 PAH. During the sampling period (T0-T18), the proportion of naphthalenes decreased and consistently declined over time, primarily for the less substituted homologs (C1-C3). Only the relative abundance of the more substituted naphthalene homolog C4 increased over time. At the end of the experiment, the relative PAH abundance progressively shifted from being dominated by two-ringed PAHs towards the larger three and four-ringed PAHs (e.g., anthracenes and pyrenes) and their substituted homologs, which had consistently increased during the exposure. The relative abundance of the anthracenes group (C0-C4) increased from 7.3% to 27.6% from T0 to T18. During all time points measured during the exposure, chrysenes and dibenzothiophenes appeared at low percentages of the total PAHs.

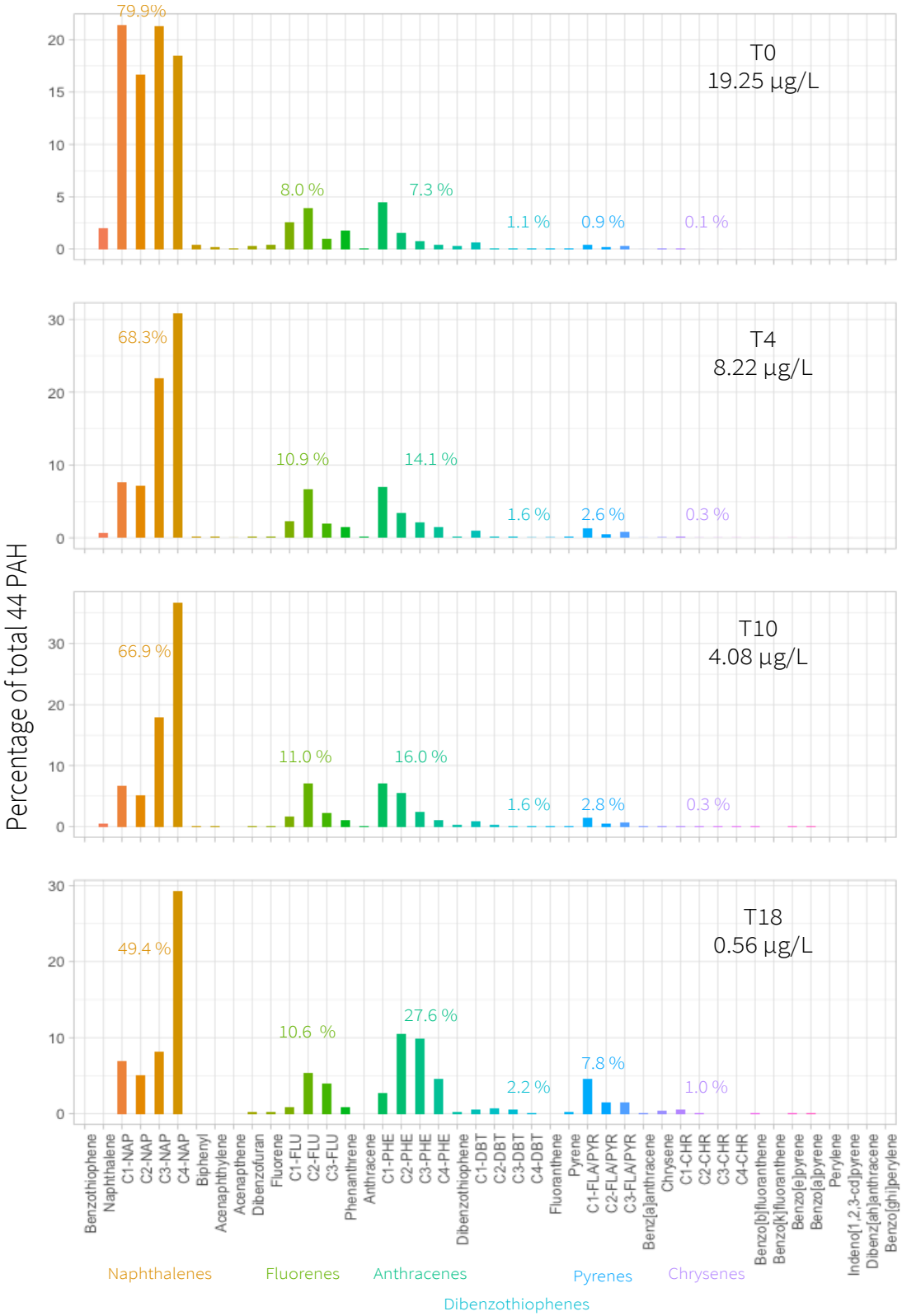

Figure 7: Representative composition of total sum of 44 PAHs of individual PAHs measured in treatment water for treatment extra high (6 g crude oil /kg gravel) over time. Composition shown for four timepoints, T0, T4, T10 and T18 (6 dpf – 24 dpf), and total PAH concentrations are listed for each. Note that the y-axis have different ranges. Parent compounds are indicated with full name, while numbers of additional carbons (e.g. methyl groups) for alkylated homologs are indicated as C1-, C2-, etc. The color-coded parent and alkylated homologs chemical groups shows the two-ringed naphthalenes, the three-ringed fluorenes, anthracenes and dibenzothiophenes, and the four-ringed pyrenes and chrysenes. Benzo[b]fluoranthene and the rest of the compounds to the right for chrysenes are all larger five – or six-ringed PAHs (Stogiannidis and Laane 2015).

3.2 Embryo mortality and development

The proportion of dead embryos or abnormal development did not show any clear dose-dependent effects (Figure 8). The highest embryo mortality at 16 dpf (T10) was observed in the low treatment with 16.30 ± 2.56% dead embryos and was significantly higher than the medium (4.66 ± 1.16%) and high treatments (5.35 ± 1.0%), respectively. The extra high treatment was just under the level of significance (p=0.067) compared to the low treatment. The highest normal embryo percentage was in treatment medium with 94.20 ± 0.81% normal embryos, followed by treatment high with 92.12 ± 1.64% and extra high with 91.99 ± 1.58% normally developed embryos. The level of the proportion of abnormal eggs was considered low (1.14 ± 0.67% in medium - 3.14 ± 1.12% in control).

At 28 dpf (T22) embryo mortality was significantly higher in the control group (15.60 ± 7.20 %) and the high treatment (14.59 ± 3.35%) compared to the medium (5.85 ± 0.41%) and extra high (7.85 ± 2.92%) treatments, respectively. Additionally, the percentage of abnormal eggs at 28 dpf was below 7% in all treatments (0.38 ± 0.38% in extra high – 6.86 ± 2.29% in medium). The medium (6.86 ± 2.29%) and high (6.69 ± 0.70%) treatments showed nevertheless significantly higher levels compared to the control (0.89 ± 0.51%), low (1.80 ± 1.05) and extra high (0.38 ± 0.38) treatments.

1

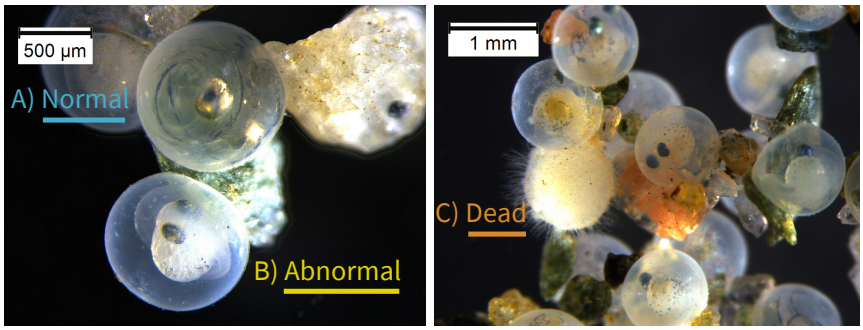

2

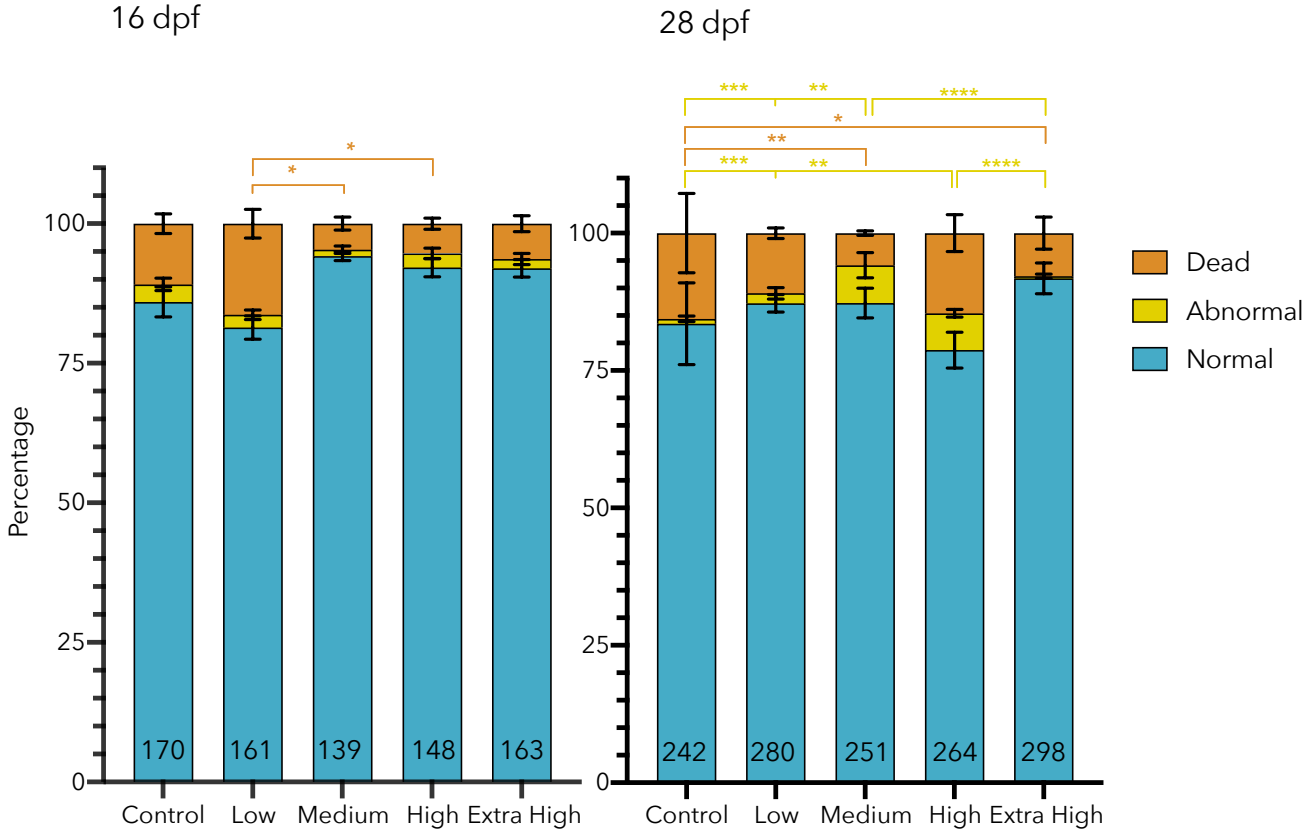

Figure 8: Egg mortality and development based on three categories: Normal, abnormal and dead embryos for two timepoints: 16 dpf (T10) and 28 dpf (T22). 1: Representative photographs of embryos during development. A) Normally developed embryo (28 dpf), B) Abnormally developed embryo (28 dpf) and C) dead embryo (24 dpf). 2: Averaged percentage of embryonic condition, categorized as normal, abnormal and dead eggs at 16 dpf (left) and 28 dpf (right) for all treatment groups. Plot values are treatment means and SEM for the three categories based on multiple larvae from each replicate (n=4) for each treatment. The numbers inside the bars indicate the total number of individuals classified per treatment. The symbol * (asterisk) indicate significant differences from the Fishers exact test. (* p ≤0.05, ** p ≤0.01, *** p ≤0.001, **** p ≤0.0001) between embryonic conditions across the five treatments.

3.3 Larval growth

There was no dose-dependent effect between treatments in measured length (Figure 9). The only statistical significant differences was at day 36, where the larvae in treatment low was significantly longer than high (p=0.0009) and extra high treatments (p=0.0125), and treatment medium longer than high (p=0.0399). Mean treatment size at (T26/32dpf) was 6.51 ± 0.031 mm in the control group, 6.69 ± 0.028 mm in low, 6.50 ± 0.030 mm in medium, 6.54

± 0.031 in high and 6.59 ± 0.031 mm in extra high treatment. The stippled line drawn between the timepoints is only an indication of variations in length measurements over time. Growth rate was calculated using equation 1 and analyzed between T26 - T36, T36 - T46, and T26 - T46 to check for nuances in growth rate (Table 1). No significant difference in growth rate between the treatments was found.

Larval length increased for all treatments from T26 to T46, except for treatment low and medium, which decreased in the period T36 to T46. There was some large variability between replicate incubators in treatment low at T46, which seems to be due to large variability in one of the incubators, in particular, causing a clear decrease in both growth rate (Table 1) and length measured between T36 and T46. The mean was 0.134 mm higher at the beginning of the experiment (T26) than at T46 for one low treatment incubators. At the last sampling (T46), the low treatment had one incubator averaged mean of 7.45 ± 0.138 mm and another with 6.58 ± 0.094 mm. This large variability pulled down the treatment mean from 7.26 ± 0.042 at T36 to 7.05 ± 0.059 mm at T46.

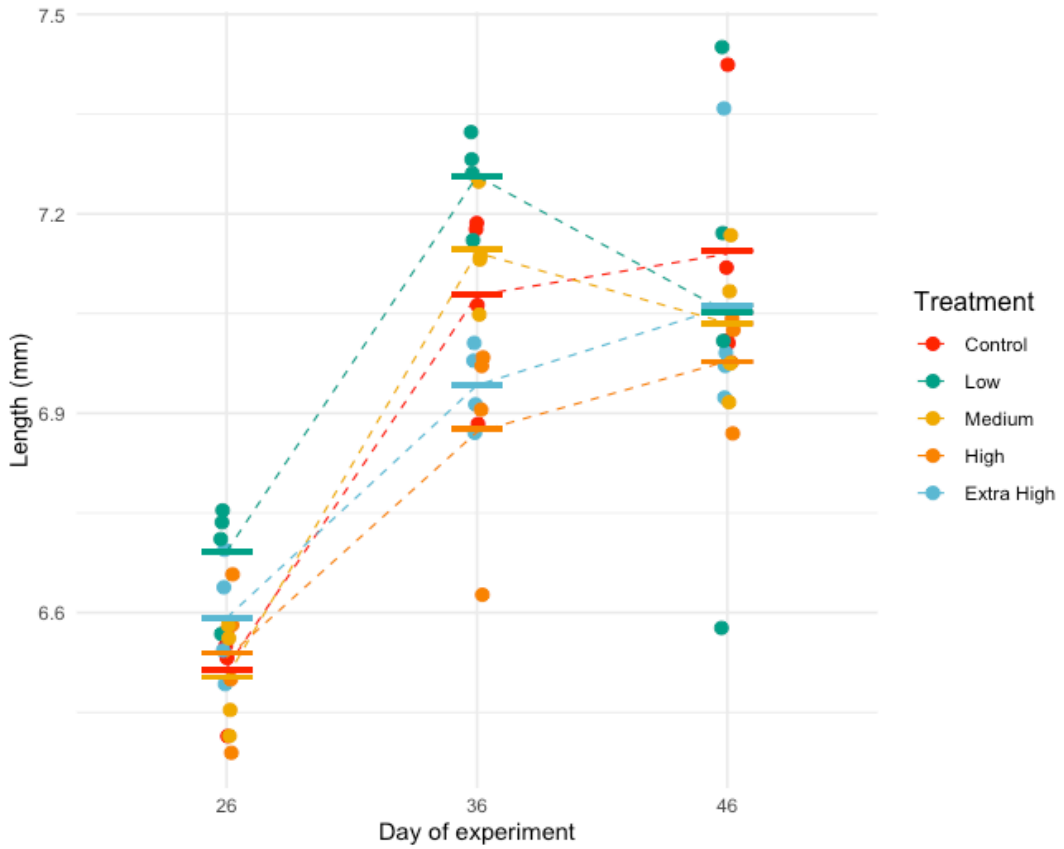

Figure 9: Length measurement (in mm) from randomly collected larvae at day T26 (32 dpf), T36 (42 dpf) and 46 (52 dpf) plotted over time. 30 larvae per incubator were measured at each timepoint. Each dot represents one incubator average per treatment (n=30). Vertical line is treatment means based on four replicate incubators. The incubator averaged length measurements displayed as dots are of different individuals between timepoints, used to give representative samples across treatments since repeated length measurements over time were not possible. The stippled line between timepoints illustrates changes in treatment means. Length data is log-transformed for the statistical calculations.

Table 1: Growth rate calculated between T26 – T46, T26 – T36 and T36-T46 for the different treatments using equation 1. The table presents treatment means based on incubator averaged values (n=4) ± SEM.

Treatment	T26 - T46	T26 - T36	T36 - T46
Control	0.46 ± 0.07	0.82 ± 0.05	0.09 ± 0.16
Low	0.26 ± 0.15	0.81 ± 0.10	-0.29 ± 0.28
Medium	0.39 ± 0.06	0.91 ± 0.08	-0.12 ± 0.10
High	0.33 ± 0.06	0.51 ± 0.17	0.16 ± 0.07
Extra High	0.34 ± 0.09	0.52 ± 0.09	0.17 ± 0.13

3.4 Cardiac activity and arrhythmia in larvae

Larvae that were randomly collected from the water column at T45 (51 dpf) exhibited significant differences in cardiac activities across treatments, but without a clear dose-dependent pattern (Figure 10). Mean cardiac activity in treatment low and medium were significantly higher than in treatment extra high ($p = 0.0231$ and $p = 0.00635$ respectively). The average cardiac activity (mean of four replicate incubators, in BPM) were 74.3 ± 0.7 in control, 83.4 ± 8.3 in low, 85.0 ± 8.6 in medium, 72.3 ± 3.0 in high and 63.4 ± 6.5 in extra high treatment. Arrhythmia measured as interbeat variability (n=20 per treatment) was assessed in the control (2.31 ± 0.49) and extra high (3.67 ± 1.01) treatments. No significant differences ($p = 0.284$) between the two treatments (control and extra high) was found, and therefore no further examinations were conducted in the remaining treatments. Additionally, no malformations (i.e., craniofacial abnormalities, body axis defects) were observed by visual assessment in any of the hatched larvae assessed for cardiotoxicity (n=100).

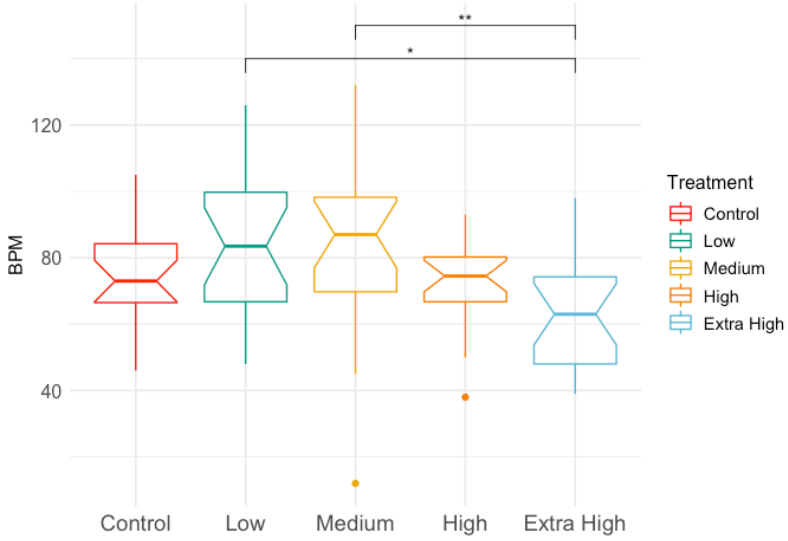

Figure 10: Cardiac activity measured per treatment (n=20) in beats per minute (BPM) at timepoint T45 (51 dpf). Each boxplot includes four incubator means calculated from 5 larvae. Significant differences from the Kruskal-Wallis test are indicated in the graph with * and ** between treatment low - extra high and medium – extra high, and the significance level was set at p-values <0.05. The boxplots represent the first and third quartile as well as the median per treatment. Outliers are displayed as dots.

3.5 Larval mortality

First, treatment low (p=0.0008) and extra high (p=0.01) had an initial density that was significantly higher than control, which represents an initial density of 180% and 119% higher than control. Secondly, there were no significant differences in the decrease in density between treatment groups (Figure 11). The first sampling at T29 (35 dpf) was set as a baseline and the treatment groups had a starting density of: Control 76.3 ± 12.1 larvae per liter, low 195.2 ± 11.3 larvae per liter, medium 87.2 ± 16.0 larvae per liter, high 81.6 ± 16.6 larvae per liter and extra high 217.3 ± 49.57. The reason for the higher SEM for treatment extra high was that one of the replicate incubators (B1), in particular, had a high incubator average density. All treatment groups decrease in larval density from T32 and until the end of the experiment. Between the two last samplings from T44 until T51, all treatments showed a sharp and significant decrease in density.

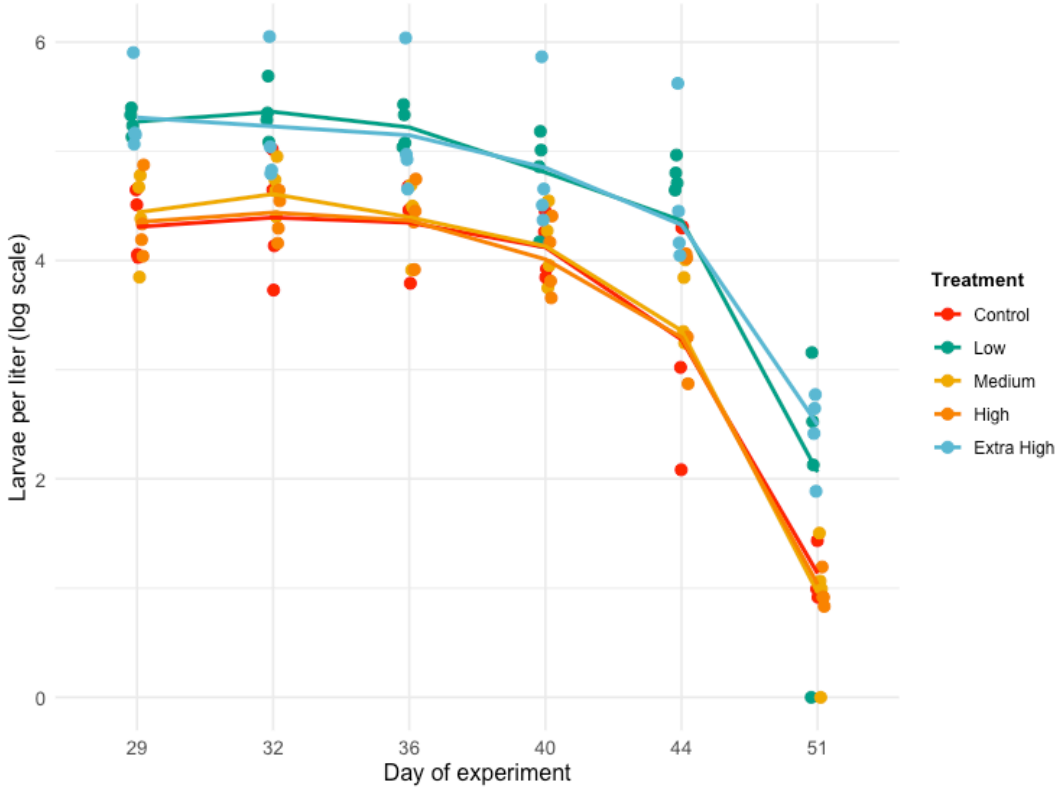

Figure 11: The effect of WSF crude oil exposure on mortality displayed as larval density (larvae per liter) on a log-scale from T29 until T51 (35 dpf - 57 dpf). The average larvae per liter data is displayed as dots for each incubator (n=4) at the six sampling timepoints. Colors indicate the different treatment groups. The line represents the changes in treatments mean (based on four replicate incubator means) between timepoints.

4 Discussion

The objective of this study was to investigate the sublethal effects and mortality of WSF of crude oil on the embryonic and larval development of ELS capelin. We hypothesized a dose-dependent decrease in growth, impaired cardiac activity, and an increase in mortality for the higher exposure doses. However, the results investigated and presented in this thesis showed a lack of dose-dependent effects for any of the biological responses analyzed during the study. Capelin ELS are seemingly less sensitive to embryonic crude oil exposure than several other species (Incardona et al. 2009; Nahrgang et al. 2016; Xu et al. 2018). In general, it is important to exhibit caution when comparing ELS crude oil studies and their cause/effect relations. The preparation of oil mixture and the oil type, compound potency or relative abundance, differences in analytical techniques, exposure duration, statistical analyses (e.g., thresholds, LOEC and EC_{50}) and differences in species sensitivity can all lead to a great range of effect concentrations recorded in marine teleosts (Nahrgang et al. 2016; Pasparakis et al. 2019). Additionally, the sum of 44 PAHs makes up a small percentage of the total hydrocarbons of the WSF of crude oil, and the primary causative agent for ELS fish toxicity is not shown to be limited to PAHs (Meador and Nahrgang 2019). Further, the bioaccumulation of compounds internally is mixture, species, and life stage specific (Meador et al. 2008). Despite the vast number of PAH toxicity studies conducted, a limited number of these studies report the actual amount of compounds bioaccumulated in fish ELS (El-Amrani et al. 2013; Incardona et al. 2012; Sørensen et al. 2017) and in these few cases, only a small set of crude oil related compounds were quantified. The lack of appropriate chemistry data causes difficulties when comparing ELS crude oil studies as well, because of the unknown fraction of bioaccumulated compounds.

Therefore, the discussion of the results from this embryonic exposure of capelin will be discussed primarily in relation to the unpublished work of Bender et al. (in preparation). Indeed, the study by Bender et al. is conducted on the cold water species polar cod (*Boreogadus saida*), with the same setup for exposure regarding the experimental design using identical oiled gravel columns and type of oil (Kobbe oil, SINTEF) as in this experiment. The polar cod treatments consisted of one control group (0 g crude oil/kg gravel) and three crude oil exposure groups (0.19 g/kg, 0.75 g/kg, and 3 g/kg). This is the exact concentrations used in the capelin experiment, except for extra high treatment with 6 g/kg. The total PAH levels the polar cod embryos were exposed to within the first four days of

exposure was in the 5-237 ng/L range (i.e., at least 80 fold lower than seen in the present study). In comparison to Bender et al. (in preparation), the exposure of capelin embryos commenced 6 dpf, whereas the polar cod embryos were exposed 0 dpf. The findings in the study from Bender et al. (in preparation) showed that crude oil exposed polar cod larvae were afflicted with deformities of the jaws, eyes, and spine, and reduced heart rate. In Nahrgang et al. (2016) polar cod ELS study low levels of hydrocarbons (2.18 µg/L Σ26 PAH initial concentration) in the WSF of crude oil caused effects including dose-dependent spine curvature, yolk sac alterations, and reduced length. Both studies demonstrate a high sensitivity of polar cod early life stages.

4.1 Chemical analysis

A series of studies have documented that exposure to dissolved PAHs from crude oil are directly toxic to fish embryos at low µg/L aqueous concentrations (Carls et al. 1999; Heintz et al. 1999; Incardona et al. 2009; Nelson et al. 2016). In this experiment, capelin embryos were exposed to crude oil and analyzed for Σ44 PAH in the WSF, which was in the 0.53-19.25 µg/L range during the first four days of exposure. The total sum of PAHs measured on day 0 of the exposure for the extra high treatment was about 200 fold higher than >0.1 µg/L, which is the level considered hazardous for fish ELS following an oil spill (Hodson 2017). The concentration of total sum PAHs measured during the 2010 DWHOS was reported to be as high as 189 µg/L, and the years following EVOS 0.13-126.63 µg/L measured in Prince William Sound, Alaska (Boehm et al. 2007). Embryos in this study got exposed to values in the lower EVOS range. During the exposure of capelin embryos from 6 dpf, until 25 dpf, the Σ44 PAH concentration decreased over time as intended (Carls and Meador 2009; Gardiner et al. 2013). The continuous weathering caused an overall shift in the relative proportions of waterborne PAHs composition from predominantly two-ring (naphthalenes) to three-ring PAHs (e.g. anthracenes). The reason for this is that smaller PAHs are released more rapidly from the crude oil system than larger and more substituted compounds (Incardona et al. 2004). Additionally, low temperatures lead to slower solubilization of the water-soluble fraction, which can result in different concentrations of PAHs in the water over time compared to warmer temperatures (Brandvik and Faksness 2009). Bender et al. (in preparation) used water temperatures of 0.5°C and 2.5°C in comparison to 5.5°C in this study. Therefore, the total sum of PAHs used as a proxy for the WSF in the capelin experiment suggested that the water concentration of oil-related compounds, especially the WSF, were

different and seemingly higher for the capelin ELS study than the comparable polar cod experiment, although nominal crude oil concentrations were identical.

Comparing crude oil toxicity studies using PAHs as a proxy for crude oil or crude oil WSF have recently been disputed by Meador and Nahrgang (2019) in a critical review. They challenge the current view on and methods used to investigate ELS fish toxicity to crude oil. According to the critical review, the basis for comparisons depend on a limited set of chemistry data, and no meaningful comparisons are possible due to the lack of evidence that PAHs are the sole toxic fraction. One example they present of a problematic methodology frequently used is that there are several methods to prepare crude oil WSF, WAF and CEWAF among other, which all can produce vastly different aqueous fractions of crude oil in regards to component concentration and profile. Meador and Nahrgang (2019) conclude that there are compounds additional to PAHs in the WSF that are likely contributing to the toxic response. The criticism presented in this review can be beneficial to consider in future research and experimental design.

4.2 Embryo mortality

One of the main toxic responses commonly observed in crude oil exposed fish ELS include mortality (Incardona and Scholz 2016; Sørhus et al. 2015). Embryo mortality or abnormal embryonic development resulting from the crude oil WSF exposure did not occur during the capelin experiment. In 2012, Frantzen et al. (2012) exposed capelin embryos to crude oil concentrations (3, 6 and 12 g crude oil/kg gravel) corresponding to initial PAH water levels ranging from 14.6 to 81.2 µg/L (Σ26 PAH). They saw a significant dose-dependent increase in embryo mortality for treatment medium (40.4 µg/L) and high (81.2 µg/L), with total mortality of approx. 75% and 90%, respectively. The concentrations of crude oil WSF, leading to increased mortality in Frantzen et al. (2012) experiment were noteworthy at least 2-fold higher than used in this experiment, supporting our findings. Comparing to this, Bender et al. (in preparation) did not see any difference in polar cod embryo mortality in crude oil treatments during the period from fertilization through gastrulation. However, during organogenesis, high oil exposure negatively affected survival in embryos.

We hypothesized that demersal eggs might have lower sensitivity than pelagic eggs to crude oil exposure due to the thicker chorion protecting from compound uptake. Similar to capelin, the Pacific herring (*Clupea pallasi*) have adhesive and demersal eggs that are covered by a

thick, three-layered chorion (Blaxter and Holliday 1963). Contrary to our hypothesis, only a few studies have shown significant developmental effects occurring at ΣPAH crude oil WSF below 1 µg/L, for one of which is herring, where ΣPAH level of 0.23 µg/L caused prolonged developmental cardiotoxicity (Incardona et al. 2015; Incardona et al. 2012). Several studies of capelin ELS sensitivity to crude oil WSF (Frantzen et al. 2012; Paine and Leggett 1992) have not found any sublethal effects on endpoints at concentrations considerably higher (Paine and Leggett: 500-5400 µg/L, Frantzen et al.: 14.6-81.2 µg/L) than for herring. One possible reason for this difference in sensitivity between fish species with demersal eggs might be due to their reproductive strategy. Capelin possesses extreme adaptations to the intertidal zone that other demersal spawners such as herring, does not. Beach-spawned eggs are subjected to severe perturbations in the physical environment compared to eggs spawned in deeper and more stable water masses (Christiansen et al. 2008). During diurnal tidal periods, they get exposed to vast and regular fluctuations in temperature and salinity, mechanical actions from waves, sunny weather and droughts (Præbel et al. 2009). The capelin eggs have evolved an array of biological and biomechanical adaptations to survive in such harsh and unpredictable physical conditions in the intertidal zone, which includes the ability to survive in a super-cooled state due to the double chorion that prevents penetration of ice crystals from the environment (Davenport and Vahl 1983; Præbel et al. 2009). In comparison, herring spawns demersal on a bottom substrate and is not exposed to such conditions as the beach-spawned demersal eggs are.

Further, it is noteworthy to mention that during the embryonic period, all samples were taken from the top of the egg-bearing substrate in the incubators. In their natural habitat, the fertilized capelin eggs become firmly attached to the substrate during spawning, and they may be buried as deep as 12–14 cm into the substrate without a marked increase in mortality (Frank and Leggett 1981). Therefore, we conclude that this sampling method did not lead to any experimental bias in regards to embryo mortality.

4.3 Larval growth and mortality

The larval stage in both nature and aquaculture industry is characterized by high and variable growth and mortality (Houde 1997; Stuart and Drawbridge 2011). Both endpoints have clear ecological relevance and encompass and integrate the effects of multiple targets of exposure (Pasparakis et al. 2019). The crude oil exposure did not cause any dose-dependent impairment

of growth, neither length measurements nor growth rate. However, there were some significant differences in length measures at experimental day 36 (42 dpf) for treatment low (0.19 g/kg) and medium (0.75 g/kg) which were significantly larger than the two exposure groups with highest crude oil concentration (high 3 g/kg and extra high 6 g/kg). In contrast, both treatment low and medium appeared to decrease in length based on treatment averaged values from T36 to T46 (Figure 9). Evidently, the larger capelin larvae seem to have died off in some of the replicate incubators in treatment low and medium in particular. However, there are no dose-dependent or other obvious explanations for this trend. Therefore, it may be concluded that the levels of crude oil WSF in the present study did not cause any effect on the larval growth. Larval mortality was generally quite low as far as T44 (50 dpf) for all treatments, even though there were some variations between the replicate incubators. In general, 60-80% of the total larvae from peak hatch at T32 remained alive at T44. The sharp increase in mortality from T44 to T51 was quite similar for all the treatments and might be caused by some unforeseen issues regarding the feeding regime of the capelin larvae. In Frantzen et al. (2012) ELS study on capelin, it was stated that the lack of observed sublethal effects might have been caused by high mortality in the treatment groups, leaving a too low number of hatched larvae to reveal any significant effects. According to the embryonic and larval mortality in this experiment, the lack of sublethal effect is most likely not due to the lack of hatched larvae surviving.

4.4 Cardiac activity

Early life stage cardiac impairment – commonly referred to as cardiotoxicity – is one of the most frequently assessed endpoints associated with oil exposure (Pasparakis et al. 2019). Cardiotoxic effects, including heart malformations, reduction in heart rate and increased heart arrhythmia are commonly used and well-studied metrics (Esbaugh et al. 2016; Incardona et al. 2014; Incardona and Scholz 2016), and occur at relatively low levels (µg/L) of aqueous PAH concentrations of crude oil (Incardona et al. 2015). The accumulation of fluid (pericardial– and yolk sac edemas), craniofacial and body defects are some of the many adverse effects of crude oil exposure that are suggested to be secondary to reduced cardiac function (Incardona et al. 2004; Incardona and Scholz 2016; Perrichon et al. 2017). Larvae malformations following embryo exposure are frequently reported, including for capelin (Paine and Leggett 1992), and are typically associated with a secondary effect of heart malformations (Adeyemo et al. 2015; Bosker et al. 2017; Incardona and Scholz 2016; Nahrgang et al. 2016). Heart

malformations at the embryonic stage are frequently associated with lower hatching rates and larval survival, and cardiac dysfunction leading to several morphological defects are suggested to be caused by exposure to PAHs (Beirão et al. 2019; Carls et al. 1999; Esbaugh et al. 2016; Incardona and Scholz 2016). Bender et al. (in preparation) observed a decrease in heart rate with increasing exposure to crude oil in newly hatched polar cod larvae (Figure 6b in appendix). They did also observe cardiac arrhythmia and a higher incidence of yolk sac edema for the larvae exposed to the highest oil treatment (i.e., 237 ng/L) (Figure 6c and 6d in appendix). In Nahrgang et al. (2016) similar polar cod study no cardiotoxic effects were found, suggesting that the levels of crude oil (0-2.18 μg/L Σ26 PAH) in that study were too low to cause any significant effects, or that the cardio-affected larvae had died at the time of sampling. Nevertheless, they found significant sublethal effects on spine curvature, yolk sac alternations, and reduced length.

In our study, we failed to detect any dose-dependent cardiac impairment or overall malformations in the hatched larvae from any treatments. In support of this, Frantzen et al. (2012) and Paine and Leggett (1992) also failed to detect developmental deformities in capelin larvae at even higher crude oil PAH concentrations. The lack of cardiotoxic effects found in this study supports the results of other measured endpoints (i.e., larval length and growth rate) since an altered cardiac function is likely to influence larval health and survival both directly and indirectly (Incardona et al. 2009; Mager et al. 2014). Direct effects encompass effects on heart development, cardiac function and swimming performance. The indirect effect includes an effect on basal metabolism, energy budget, growth, overall health, and size-dependent predation (Incardona et al. 2015). Neither a dose-dependent increase in mortality, reduction in growth, nor any malformations were found for any of the experiments conducted in this study. Sublethal effects which include cardiac arrhythmia, yolk sac edema, and skeletal deformities may be less pronounced in capelin embryos compared to other, potentially more sensitive fish species (Incardona et al. 2015; Incardona et al. 2012).

4.5 Species specific sensitivity to crude oil

According to Incardona et al. (2013), all values reported for pelagic species are well below the reported cardiotoxicity for zebrafish, a commonly used model species. As such, it appears that zebrafish is at least one order of magnitude less sensitive than the studied pelagic fish from the GoM. The physiological ecology of a given fish can cause different cardiac

responses. For example, species from northern latitudes (e.g., herring and haddock) typically respond to crude oil exposure with severe bradycardia (slow heart rate) or arrhythmia. These cardiac responses are not observed for species with more warm water temperature tolerances (e.g., zebrafish and mahi-mahi), whereas they typically respond with reduced contractility, and no major effects on heart rate and rhythm (Haverinen and Vornanen 2009; Incardona 2017). Noteworthy, toxicity is determined by many diverse factors, including but not limited to, exposure duration, oil type and preparation, and the inclusion or absence of additional environmentally relevant stressors (Pasparakis et al. 2019). Consequently, the possibility of comparison between differences in sensitivity among endpoints measured between different life stages and fish species may vary due to various experimental setups.

Based on studies on DWH oil toxicity, the difference between the ELS and adults is relatively modest and spans only about 1-2 orders of magnitude. However, the variation in sensitivity among species in studies on ELS varies by 2–3 orders of magnitude (Pasparakis et al. 2019). Therefore, it is essential to look at species specific toxicity, and it seems to indicate that certain species are more sensitive than others to crude oil exposure (Khursigara et al. 2017; Xu et al. 2018). For example, sheepshead minnow shows no effect on survival at concentrations as high as 99 $\mu g\ l^{-1}$ ΣPAH_{50} after 2-day exposure (Finch et al. 2017). Differently, mahi-mahi and red drum both show 50% mortality after exposure to 6.5 $\mu g\ l^{-1}$ ΣPAH_{50} for four days and <20 $\mu g\ l^{-1}$ ΣPAH_{50} for three days, respectively (Khursigara et al. 2017; Stieglitz et al. 2016a). Comparison between studies using PAHs as the main toxic compounds of crude oil or crude oil WSF, as all three studies mentioned, have as mentioned been disputed by Meador and Nahrgang (2019) critical review. They challenge the current view on fish ELS toxicity studies and claim that differences shown in species specific toxicity could be due to a difference in compounds bioaccumulated and a reflection of the unique chemical characteristics of a given type of crude oil. Additionally, after the DWHOS mahi-mahi (*Coryphaena hippurus*) appeared to be the most sensitive species tested, but that may be in part due to the comprehensive experimentation performed on this species increases the likelihood of revealing more sensitive endpoints (Pasparakis et al. 2019). Therefore, further research on ELS capelin might lead to findings of more sensitive endpoints.

4.6 Life stage specific sensitivity to crude oil

In the present study, the capelin embryos were first exposed to crude oil WSF 6 days post fertilization. The initial embryonic developmental stages used in crude oil exposure studies might affect the effect concentration and sensitivity of measured endpoints. Beirão et al. (2019) exposed capelin embryos to chemically-enhanced WAF (CEWAF), and kept the concentrations stable from 0 dpf and 6 dpf (corresponding to late organogenesis) until hatching, in contrast to our study. The hatching success was lower for embryos exposed to CEWAF at 10.4 µg/L total PAH after late organogenesis (6 dpf), in comparison to 2.8 µg/L when exposed throughout development from 0 dpf (Beirão et al. 2019). In a similar study conducted by McIntosh et al. (2010) on Atlantic herring (*Clupea harengus*), the age of the embryos was found to correlate with their sensitivity to oil negatively; those freshly fertilized were most sensitive. The sensitivity of embryos was greatest during the first 24 h after fertilization, and no visible effect was found for embryos exposed at 11 dpf (McIntosh et al. 2010). Paine and Leggett (1992) exposed capelin to WSF crude oil in four different experiments. The first experiment measured the effects of crude oil WSF on survival and growth of embryos with exposures beginning at two different ages: 0 and 5 dpf and lasting until hatch. Findings suggested some differences in sensitivity, with an increase in hatching success for the group exposed to crude oil 5 dpf. These studies indicate that the capelin embryos show a higher sensitivity at fertilization and the first days after than later in the embryonic development. Paine and Leggett (1992) conducted a second experiment to investigate the effect of WSF on survival. The findings indicate that exposures causing lethal effects were an order of magnitude lower for larvae than for embryos, and in that matter that capelin larvae are more sensitive to crude oil WSF than embryos. Given the suggested increased sensitivity for fish embryos during the first days post fertilization (Beirão et al. 2019; McIntosh et al. 2010; Paine and Leggett 1992), our study and others commencing several days post fertilization may not discover sensitive endpoints due to the specific study design used (McIntosh et al. 2010). Noteworthy, it is important to stress that all studies mentioned have used different oil types and experimental designs, and caution should be used in comparing across studies.

4.7 Conclusion and future outlook

The experimental designed used in this study to simulate an accidental oil spill in the proximity of capelin spawning grounds used oiled gravel columns to mimic field conditions

after an oil spill. Despite the hypothesized expectations of a decrease in growth, impaired cardiac activity, and an increase in mortality with increasing concentrations of crude oil, the results of this study do not show any adverse dose-dependent effects on ELS capelin. The lack of adverse effects supports findings in previously published studies that have shown effects of crude oil WSF or CEWAF in capelin ELS only at concentrations of ΣPAHs from 2-4 fold up to 270-700 fold higher than used in this experiment (Frantzen et al. 2012; Paine and Leggett 1992; Tairova et al. 2019). In comparison to ELS of other fish species', and polar cod in particular, capelin ELS seems to be a more robust and less sensitive species. Bender et al. (in preparation) found that crude oil exposed larvae were afflicted with deformities of the jaws, eyes and spine, and reduced heart rate. In this study, capelin embryos were exposed to levels of crude oil WSF with PAH levels during the first four days of the experiment at least 80-fold higher than in the polar cod study by Bender et al. (in preparation). Importantly, even though the timeframe corresponds, the developmental stage (dpf) at start of exposure varies between these studies. One hypothesis suggested to explain this lowered sensitivity was that demersal fish eggs are less sensitive than pelagic eggs due to the eggs morphology and structure. The literature discussed in this study does not confirm this hypothesis. One suggestion is that the adaptations to survival in the intertidal zone might be a possible reason to explain why capelin ELS seems to be less sensitive than other species with demersal eggs. Given this, it would be interesting to investigate the difference between the demersal eggs herring and capelin have to gain more knowledge about what distinguishes them in regards to the ELS sensitivity to crude oil. Further, the adhesive membrane covering haddock egg has been shown to contribute to the interaction with oil droplets and leading to profound consequences for toxicity (Morrison et al. 1999; Sørensen et al. 2017). Therefore, it could be interesting to investigate whether the adhesive capelin eggs show a similarly increased uptake of PAHs due to oil droplets adhesion to the chorion.

References

Abdel-Shafy HI, Mansour MSM. 2016. A review on polycyclic aromatic hydrocarbons: Source, environmental impact, effect on human health and remediation. Egyptian Journal of Petroleum. 25(1):107-123.

Adeyemo OK, Kroll KJ, Denslow ND. 2015. Developmental abnormalities and differential expression of genes induced in oil and dispersant exposed *Menidia beryllina* embryos. Aquatic Toxicology. 168:60-71.

Almeda R, Baca S, Hyatt C, Buskey EJ. 2014. Ingestion and sublethal effects of physically and chemically dispersed crude oil on marine planktonic copepods. Ecotoxicology. 23(6):988-1003.

Anderson CM, Mayes M, LaBelle R. 2012. Update of occurence rates for offshore oil spills. Herndon VA: OSC report.

Behrens JW, Præbel K, Steffensen JF. 2006. Swimming energetics of the Barents Sea capelin (*Mallotus villosus*) during the spawning migration period. Journal of Experimental Marine Biology and Ecology. 331(2):208-216.

Beirão J, Baillon L, Litt MA, Langlois VS, Purchase CF. 2019. Impact of crude oil and the dispersant Corexit™ EC9500A on capelin (*Mallotus villosus*) embryo development. Marine Environmental Research. 147:90-100.

Bence AE, Kvenvolden KA, Kennicutt MC. 1996. Organic geochemistry applied to environmental assessment of Prince William Sound, Alaska, after the *Exxon Valdrez* oil spill - a review. Organic geochemistry. 24(1):7-42.

Beyer J, Trannum HC, Bakke T, Hodson PV, Collier TK. 2016. Environmental effects of the Deepwater Horizon oil spill: A review. Marine Pollution Bulletin. 110(1):28-51.

Blaxter JHS, Holliday FGT. 1963. The behaviour and physiology of herring and other clupeids. Russel FS, editor. London: Academic Press.

Boehm PD, Neff JM, Page DS. 2007. Assessment of polycyclic aromatic hydrocarbon exposure in the waters of Prince William Sound after the Exxon Valdez oil spill: 1989–2005. Marine Pollution Bulletin. 54(3):339-356.

Bosker T, van Balen L, Walsh B, Sepúlveda MS, DeGuise S, Perkins C, Griffitt RJ. 2017. The combined effect of Macondo oil and corexit on sheepshead minnow (*Cyprinodon variegatus*) during early development. Journal of Toxicology and Environmental Health, Part A. 80(9):477-484.

Brandvik PJ, Faksness L-G. 2009. Weathering processes in Arctic oil spills: Meso-scale experiments with different ice conditions. Cold Regions Science and Technology. 55(1):160-166.

Brinkworth LC, Hodson PV, Tabash S, Lee P. 2003. CYP1A Induction and Blue SAC Disease in Early Developmental Stages of Rainbow Trout (*Oncorhynchus Mykiss*) Exposed to Retene. Journal of Toxicology and Environmental Health, Part A. 66(7):627-646.

Brown ED. 2002. Life history, distribution, and size structure of Pacific capelin in Prince William Sound and the northern Gulf of Alaska. ICES Journal of Marine Science. 59(5):983-996.

Carls M, Meador J. 2009. A Perspective on the Toxicity of Petrogenic PAHs to Developing Fish Embryos Related to Environmental Chemistry. Human and Ecological Risk Assessment - Human and Ecological Risk Assessment. 15:1084-1098.

Carls MG, Rice SD, Hose JE. 1999. Sensitivity of fish embryos to weathered crude oil: Part I. Low-level exposure during incubation causes malformations, genetic damage, and mortality in larval pacific herring (*Clupea pallasi*). Environmental Toxicology and Chemistry. 18(3):481-493.

Chakraborty R, Borglin S, Dubinsky E, Andersen G, Hazen T. 2012. Microbial Response to the MC-252 Oil and Corexit 9500 in the Gulf of Mexico. Frontiers in Microbiology. 3(357).

Champine RD, Morris R, Elder S. 2019. The melting Arctic is now open for business. National Geographic Magazine.

Cherr GN, Fairbairn E, Whitehead A. 2017. Impacts of Petroleum-Derived Pollutants on Fish Development. Annual Review of Animal Biosciences. 5(1):185-203.

Christiansen JS, Præbel K, Siikavuopio SI, Carscadden JE. 2008. Facultative semelparity in capelin *Mallotus villosus* (Osmeridae)-an experimental test of a life history phenomenon in a sub-arctic fish. Journal of Experimental Marine Biology and Ecology. 360(1):47-55.

Cram S, Siebe C, Ortíz-Salinas R, Herre A. 2004. Mobility and Persistence of Petroleum Hydrocarbons in Peat Soils of Southeastern Mexico. Soil and Sediment Contamination: An International Journal. 13(5):341-360.

Davenport J, Stene A. 1986. Freezing resistance, temperature and salinity tolerance in eggs, larvae and adults of capelin, *Mallotus villosus*, from Balsfjord. Journal of the Marine Biological Association of the United Kingdom. 66(1):145-157.

Davenport J, Vahl O. 1983. Desiccation resistanse in the eggs of the capelin *Mallotus villosus* Astarte: Journal of Arctic Biology. 12(2):35-37.

Donkin P, Smith EL, Rowland SJ. 2003. Toxic Effects of Unresolved Complex Mixtures of Aromatic Hydrocarbons Accumulated by Mussels, *Mytilus edulis*, from Contaminated Field Sites. Environmental Science & Technology. 37(21):4825-4830.

Eguíluz VM, Fernández-Gracia J, Irigoien X, Duarte CM. 2016. A quantitative assessment of Arctic shipping in 2010–2014. Scientific Reports. 6(1):30682.

El-Amrani S, Sanz-Landaluze J, Guinea J, Cámara C. 2013. Rapid determination of polycyclic aromatic hydrocarbons (PAHs) in zebrafish eleutheroembryos as a model for the evaluation of PAH bioconcentration. Talanta. 104:67-74.

Esbaugh AJ, Mager EM, Stieglitz JD, Hoenig R, Brown TL, French BL, Linbo TL, Lay C, Forth H, Scholz NL et al. 2016. The effects of weathering and chemical dispersion on Deepwater Horizon crude oil toxicity to mahi-mahi (*Coryphaena hippurus*) early life stages. Science of The Total Environment. 543:644-651.

Faksness L-G, Brandvik PJ. 2008. Distribution of water soluble components from oil encapsulated in Arctic sea ice: Summary of three field seasons. Cold Regions Science and Technology. 54(2):106-114.

Farrington JW, Quinn JG. 2015. “Unresolved Complex Mixture” (UCM): A brief history of the term and moving beyond it. Marine Pollution Bulletin. 96(1):29-31.

Finch BE, Marzooghi S, Di Toro DM, Stubblefield WA. 2017. Phototoxic potential of undispersed and dispersed fresh and weathered Macondo crude oils to Gulf of Mexico Marine Organisms. Environmental Toxicology and Chemistry. 36(10):2640-2650.

Fingas M. 2015. Introduction to Oil Chemistry and Properties. In: Fingas M, editor. Handbook of Oil Spill Science and Technology. Hoboken, New Jersey: John Wiley & Sons, Inc. p. 51-77.

Frantzen M, Falk-Petersen IB, Nahrgang J, Smith TJ, Olsen GH, Hangstad TA, Camus L. 2012. Toxicity of crude oil and pyrene to the embryos of beach spawning capelin (*Mallotus villosus*). Aquatic Toxicology. 108:42-52.

Fridgeirsson E. 1976. Observations on spawning behaviour and embryonic development of the Icelandic capelin. Rit Fiskideildar. 5(4):1-34.

Gardiner WW, Word JQ, Word JD, Perkins RA, McFarlin KM, Hester BW, Word LS, Ray CM. 2013. The acute toxicity of chemically and physically dispersed crude oil to key arctic species under arctic conditions during the open water season. Environmental Toxicology and Chemistry. 32(10):2284-2300.

Gjøsæter H. 1998. The population biology and exploitation of capelin (*Mallotus villosus*) in the barents sea. Sarsia. 83(6):453-496.

Gjøsæter H, Bogstad B, Tjelmeland S. 2009. Ecosystem effects of the three capelin stock collapses in the Barents Sea. Marine Biology Research. 5(1):40-53.

Gjøsæter H, Gjøsæter J. 1986. Observations on the embryonic development of capelin (*Mallotus villosus* Müller) from the Barents Sea. Fiskeridirektoratets Skrifter Serie Havundersøkelser. 18:59-68.

Gjøsæter H, Ushakov NG, Prozokevich DV. 2011. Capelin. In: Jakobsen T, Ozhigin VK, editors. The Barents Sea Ecosystem, Resources, Management Half a century of Russian - Norwegian cooperation. Trondheim: Tapir Academic Press. p. 215-225.

Hansen BH, Sørensen L, Carvalho PA, Meier S, Booth AM, Altin D, Farkas J, Nordtug T. 2018. Adhesion of mechanically and chemically dispersed crude oil droplets to eggs of Atlantic cod (*Gadus morhua*) and haddock (*Melanogrammus aeglefinus*). Science of the Total Environment. 640-641:138-143.

Haverinen J, Vornanen M. 2009. Responses of Action Potential and K+ Currents to Temperature Acclimation in Fish Hearts: Phylogeny or Thermal Preferences? Physiological and biochemical zoology : PBZ. 82:468-482.

Heintz RA. 2007. Chronic exposure to polynuclear aromatic hydrocarbons in natal habitats leads to decreased equilibrium size, growth, and stability of pink salmon populations. Integrated Environmental Assessment and Management. 3(3):351-363.

Heintz RA, Rice SD, Wertheimer AC, Bradshaw RF, Thrower FP, Joyce JE, Short JW. 2000. Delayed effects on growth and marine survival of pink salmon *Oncorhynchus gorbuscha* after exposure to crude oil during embryonic development. Marine Ecology Progress Series. 208:205-216.

Heintz RA, Short JW, Rice SD. 1999. Sensitivity of fish embryos to weathered crude oil: Part II. Increased mortality of pink salmon (*Oncorhynchus gorbuscha*) embryos incubating downstream from weathered Exxon valdez crude oil. Environmental Toxicology and Chemistry. 18(3):494-503.

Hicken CE, Linbo TL, Baldwin DH, Willis ML, Myers MS, Holland L, Larsen M, Stekoll MS, Rice SD, Collier TK et al. 2011. Sublethal exposure to crude oil during embryonic development alters cardiac morphology and reduces aerobic capacity in adult fish. Proceedings of the National Academy of Sciences. 108(17):7086.

Hodson P. 2017. The Toxicity to Fish Embryos of PAH in Crude and Refined Oils. Archives of Environmental Contamination and Toxicology. 73.

Hop H, Gjøsæter H. 2013. Polar cod (*Boreogadus saida*) and capelin (*Mallotus villosus*) as key species in marine food webs of the Arctic and the Barents Sea. Marine Biology Research. 9(9):878-894.

Houde E. 1997. Patterns and trends in larval-stage growth and mortality of teleost fish*. Journal of Fish Biology. 51:52-83.

Huse G, Ellingsen I. 2008. Capelin migrations and climate change - a modelling analysis. Climate Change. 87(1-2):177-197.

Incardona JP. 2017. Molecular Mechanisms of Crude Oil Developmental Toxicity in Fish. Archives of Environmental Contamination and Toxicology. 73(1):19-32.

Incardona JP, Carls MG, Day HL, Sloan CA, Collier TK, Scholz NL. 2009. Cardiac Arrhythmia Is the Primary Response of Embryonic Pacific Herring (*Clupea pallasi*) Exposed to Crude Oil during Weathering. Environmental Science & Technology. 43:201-207.

Incardona JP, Carls MG, Holland L, Linbo TL, Baldwin DH, Myers MS, Peck KA, Tagal M, Rice SD, Scholz NL. 2015. Very low embryonic crude oil exposures cause lasting cardiac defects in salmon and herring. Scientific Reports. 5:13499.

Incardona JP, Collier TK, Scholz NL. 2004. Defects in cardiac function precede morphological abnormalities in fish embryos exposed to polycyclic aromatic hydrocarbons. Toxicology and Applied Pharmacology. 196(2):191-205.

Incardona JP, Collier TK, Scholz NL. 2011. Oil spills and fish health: exposing the heart of the matter. Journal of Exposure Science & Environmental Epidemiology. 21(1):3-4.

Incardona JP, Gardner LD, Linbo TL, Brown TL, Esbaugh AJ, Mager EM, Stieglitz JD, French BL, Labenia JS, Laetz CA et al. 2014. Deepwater Horizon crude oil impacts the developing hearts of large predatory pelagic fish. Proceedings of the National Academy of Sciences. 111(15):E1510-1518.

Incardona JP, Scholz NL. 2016. The influence of heart developmental anatomy on cardiotoxicity-based adverse outcome pathways in fish. Aquatic Toxicology. 177:515-525.

Incardona JP, Swarts TL, Edmunds RC, Linbo TL, Aquilina-Beck A, Sloan CA, Gardner LD, Block BA, Scholz NL. 2013. Exxon Valdez to Deepwater Horizon: Comparable toxicity of both crude oils to fish early life stages. Aquatic Toxicology. 142-143:303-316.

Incardona JP, Vines CA, Anulacion BF, Baldwin DH, Day HL, French BL, Labenia JS, Linbo TL, Myers MS, Olson OP et al. 2012. Unexpectedly high mortality in Pacific herring embryos exposed to the 2007 *Cosco Busan* oil spill in San Francisco Bay. Proceedings of the National Academy of Sciences. 109(2):E51.

Johansen JL, Esbaugh AJ. 2017. Sustained impairment of respiratory function and swim performance following acute oil exposure in a coastal marine fish. Aquatic Toxicology. 187:82-89.

Jurelevicius D, Alvarez VM, Marques JM, de Sousa Lima LRF, Dias FdA, Seldin L. 2013. Bacterial Community Response to Petroleum Hydrocarbon Amendments in Freshwater, Marine, and Hypersaline Water-Containing Microcosms. Applied and Environmental Microbiology. 79(19):5927-5935.

Khursigara AJ, Perrichon P, Martinez Bautista N, Burggren WW, Esbaugh AJ. 2017. Cardiac function and survival are affected by crude oil in larval red drum, *Sciaenops ocellatus*. Science of The Total Environment. 579:797-804.

Laurel BJ, Copeman LA, Iseri P, Spencer ML, Hutchinson G, Nordtug T, Donald CE, Meier S, Allan SE, Boyd DT et al. 2019. Embryonic Crude Oil Exposure Impairs Growth and Lipid Allocation in a Keystone Arctic Forage Fish. iScience. 19:1101-1113.

Lønning S, Kjørsvik E, Falk-Petersen IB. 1988. A comparative study of pelagic and demersal eggs from common marine fishes in Northern Norway. Sarsia. 73(1):49-60.

Mager EM, Esbaugh AJ, Stieglitz JD, Hoenig R, Bodinier C, Incardona JP, Scholz NL, Benetti DD, Grosell M. 2014. Acute embryonic or juvenile exposure to Deepwater Horizon crude oil impairs the swimming performance of mahi-mahi (*Coryphaena hippurus*). Environmental Science & Technology. 48(12):7053-7061.

Mager EM, Pasparakis C, Schlenker LS, Yao Z, Bodinier C, Stieglitz JD, Hoenig R, Morris JM, Benetti DD, Grosell M. 2017. Assessment of early life stage mahi-mahi windows of sensitivity during acute exposures to Deepwater Horizon crude oil. Environmental Toxicology and Chemistry. 36(7):1887-1895.

McClain CR, Nunnally C, Benfield MC. 2019. Persistent and substantial impacts of the Deepwater Horizon oil spill on deep-sea megafauna. Royal Society Open Science. 6(8):191164.

McIntosh S, King T, Wu D, Hodson PV. 2010. Toxicity of dispersed weathered crude oil to early life stages of Atlantic herring (*Clupea harengus*). Environmental Toxicology and Chemistry. 29(5):1160-1167.

McNicholl DG, Davoren GK, Reist JD. 2018. Life history variation across latitudes: observations between capelin (*Mallotus villosus*) from Newfoundland and the eastern Canadian Arctic. Polar Biology. 41(4):643-651.

Meador JP, McCarty LS, Escher BI, Adams WJ. 2008. 10th Anniversary Critical Review: The tissue-residue approach for toxicity assessment: concepts, issues, application, and recommendations. Journal of Environmental Monitoring. 10(12):1486-1498.

Meador JP, Nahrgang J. 2019. Characterizing Crude Oil Toxicity to Early-Life Stage Fish Based On a Complex Mixture: Are We Making Unsupported Assumptions? Environ Sci Technol. 53(19):11080-11092.

Melbye AG, Brakstad OG, Hokstad JN, Gregersen IK, Hansen BH, Booth AM, Rowland SJ, Tollefsen KE. 2009. Chemical and toxicological characterization of an unresolved complex mixture-rich biodegraded crude oil. Environmental Toxicology and Chemistry. 28(9):1815-1824.

Miller BS, Kendall Jr. AW. 2009. Early life history of marine fishes. Los Angeles University of California Press.

Mishra AK, Kumar GS. 2015. Weathering of Oil Spill: Modeling and Analysis. Aquatic Procedia. 4:435-442.

Morrison C, Bird C, O'Neil D, Leggiadro C, Martin-Robichaud D, Rommens M, Waiwood K. 1999. Structure of the egg envelope of the haddock, *Melanogrammus aeglefinus*, and effects of microbial colonization during incubation. Canadian Journal of Zoology. 77(6):890-901.

Nahrgang J, Bender ML, Meier S, Nechev J, Berge J, Frantzen M. 2019. Growth and metabolism of adult polar cod (*Boreogadus saida*) in response to dietary crude oil. Ecotoxicology and Environmental Safety. 180:53-62.

Nahrgang J, Dubourg P, Frantzen M, Storch D, Dahlke F, Meador JP. 2016. Early life stages of an arctic keystone species (*Boreogadus saida*) show high sensitivity to a water-soluble fraction of crude oil. Environmental Pollution. 218:605-614.

National Research Council. 2003. Oil in the Sea III: Inputs, Fates, and Effects. Washington (DC): National Academies Press (US).

Nelson D, Heuer RM, Cox GK, Stieglitz JD, Hoenig R, Mager EM, Benetti DD, Grosell M, Crossley DA. 2016. Effects of crude oil on in situ cardiac function in young adult mahi–mahi (*Coryphaena hippurus*). Aquatic Toxicology. 180:274-281.

Nelson D, Stieglitz JD, Cox GK, Heuer RM, Benetti DD, Grosell M, Crossley DA. 2017. Cardio-respiratory function during exercise in the cobia, Rachycentron canadum: The impact of crude oil exposure. Comparative Biochemistry and Physiology Part C: Toxicology & Pharmacology. 201:58-65.

Novikov MA, Titov O, V, Olsen E. 2011. Shipping. In: Jakobsen T, Ozhigin VK, editors. The Barents Sea Ecosystem, Resources, Management Half a century of Russian - Norwegian cooperation. Trondheim: Tapir Academic Press. p. 672-678.

Olsen GH, Klok C, Hendriks AJ, Geraudie P, De Hoop L, De Laender F, Farmen E, Grosvik BE, Hansen BH, Hjorth M et al. 2013. Toxicity data for modeling impacts of oil components in an Arctic ecosystem. Marine Environmental Research. 90:9-17.

Paine MD, Leggett WC. 1992. Effects of Hibernia Crude Oil on Capelin (*Mallotus villosus*) Embryos and Larvae. Marine Environmental Research. 33(3):159-187.

Pasparakis C, Esbaugh AJ, Burggren W, Grosell M. 2019. Impacts of deepwater horizon oil on fish. Comparative Biochemistry and Physiology - Part C: Toxicology & Pharmacology 224:108558.

Penton PM, Davoren GK. 2013. A common garden experiment on capelin (*Mallotus villosus*) early life history stages to examine use of beach and deep-water spawning habitats. Journal of Experimental Marine Biology and Ecology. 439:54-60.

Perrichon P, Grosell M, Burggren WW. 2017. Heart Performance Determination by Visualization in Larval Fishes: Influence of Alternative Models for Heart Shape and Volume. Frontiers in Physiology. 8:464.

Petersen K, Hultman MT, Rowland SJ, Tollefsen KE. 2017. Toxicity of organic compounds from unresolved complex mixtures (UCMs) to primary fish hepatocytes. Aquatic Toxicology. 190:150-161.

Peterson CH, Rice SD, Short JW, Esler D, Bodkin JL, Ballachey BE, Irons DB. 2003. Long-Term Ecosystem Response to the Exxon Valdez Oil Spill. Science. 302(5653):2082-2086.

Pinheiro J, Bates D, DebRoy S. 2020. Linear and Nonlinear Mixed Effects Models. R Core Team.

Præbel K, Christiansen JS, Fevolden S-E. 2009. Temperature and salinity conditions in a sub-Arctic intertidal spawning habitat for capelin. Marine Biology Research. 5(5):511-514.

Rice SD, Thomas RE, Carls MG, Heintz RA, Wertheimer AC, Murphy ML, Short JW, Moles A. 2001. Impacts to Pink Salmon Following the Exxon Valdez Oil Spill: Persistence, Toxicity, Sensitivity, and Controversy. Reviews in Fisheries Science. 9(3):165-211.

Rose GA. 2005. Capelin (*Mallotus villosus*) distribution and climate: a sea «canary» for marine ecosystem change. ICES Journal of Marine Science 62(7):1524-1530.

Rossi B. 2013. Summary Report and Recommendations on the Prevention of Marine Oil Pollution in the Arctic.

Smith LC, Stephenson SR. 2013. New Trans-Arctic shipping routes navigable by midcentury. Proceedings of the National Academy of Sciences. 110(13):E1191-1195.

Speight JG. 2014. The Chemistry and Technology of Petroleum. Boca Raton: Taylor & Francis Group, LLC.

Stieglitz JD, Mager EM, Hoenig RH, Alloy M, Esbaugh AJ, Bodinier C, Benetti DD, Roberts AP, Grosell M. 2016a. A novel system for embryo-larval toxicity testing of pelagic fish: Applications for impact assessment of Deepwater Horizon crude oil. Chemosphere. 162:261-268.

Stieglitz JD, Mager EM, Hoenig RH, Benetti DD, Grosell M. 2016b. Impacts of Deepwater Horizon crude oil exposure on adult mahi-mahi (*Coryphaena hippurus*) swim performance. Environmental Toxicology and Chemistry. 35(10):2613-2622.

Stogiannidis E, Laane R. 2015. Source Characterization of Polycyclic Aromatic Hydrocarbons by Using Their Molecular Indices: An Overview of Possibilities. Reviews of Environmental Contamination and Toxicology. 234:49-133.

Stuart KR, Drawbridge M. 2011. The effect of light intensity and green water on survival and growth of cultured larval California yellowtail (*Seriola lalandi*). Aquaculture. 321(1-2):152-156.

Sutton PA, Lewis CA, Rowland SJ. 2005. Isolation of individual hydrocarbons from the unresolved complex hydrocarbon mixture of a biodegraded crude oil using preparative capillary gas chromatography. Organic Geochemistry. 36(6):963-970.

Sørensen L, Meier S, Mjøs SA. 2016. Application of gas chromatography/tandem mass spectrometry to determine a wide range of petrogenic alkylated polycyclic aromatic hydrocarbons in biotic samples. Rapid Communications in Mass Spectrometry. 30(18):2052-2058.

Sørensen L, Sørhus E, Nordtug T, Incardona JP, Linbo TL, Giovanetti L, Karlsen O, Meier S. 2017. Oil droplet fouling and differential toxicokinetics of polycyclic aromatic hydrocarbons in embryos of Atlantic haddock and cod. PLoS One. 12(7):e0180048.

Sørhus E, Edvardsen RB, Karlsen Ø, Nordtug T, van der Meeren T, Thorsen A, Harman C, Jentoft S, Meier S. 2015. Unexpected Interaction with Dispersed Crude Oil Droplets Drives Severe Toxicity in Atlantic Haddock Embryos. PLoS One. 10(4):e0124376.

Tairova Z, Frantzen M, Mosbech A, Arukwe A, Gustavson K. 2019. Effects of water accommodated fraction of physically and chemically dispersed heavy fuel oil on beach spawning capelin (*Mallotus villosus*). Marine Environmental Research. 147:62-71.

Tarnecki JH, Patterson WF. 2015. Changes in Red Snapper Diet and Trophic Ecology Following the Deepwater Horizon Oil Spill. Marine and Coastal Fisheries. 7(1):135-147.

Vilhjálmsson H. 1994. The Icelandic capelin stock. Capelin, *Mallotus villosus* (Müller) in the Iceland-Greenland-Jan Mayen area. Marine Research Institute Reykjavík. 13(1):1-281.

Vilhjálmsson H. 2002. Capelin (*Mallotus villosus*) in the Iceland–East Greenland–Jan Mayen ecosystem. ICES Journal of Marine Science. 59:870-883.

Wang Z, Stout SA, Fingas M. 2006. Forensic Fingerprinting of Biomarkers for Oil Spill Characterization and Source Identification. Environmental Forensics. 7(2):105-146.

Wickham H. 2016. ggplot2: Elegant Graphics for Data Analysis. New York: Springer-Verlag.

Xu EG, Magnuson JT, Diamante G, Mager E, Pasparakis C, Grosell M, Roberts AP, Schlenk D. 2018. Changes in microRNA–mRNA Signatures Agree with Morphological, Physiological, and Behavioral Changes in Larval Mahi-Mahi Treated with Deepwater Horizon Oil. Environmental Science & Technology. 52(22):13501-13510.

Yim UH, Hong SH, Shim WJ. 2007. Distribution and characteristics of PAHs in sediments from the marine environment of Korea. Chemosphere. 68(1):85-92.

Appendix

Appendix Table 1: Concentrations of the 44 PAH analytes (ng/L) measured in the exposure water at four different timepoints: T0 (6 dpf), T4 (10 dpf), T10 (16 dpf) and T18 (24 dpf). The lower limit of detection (LOD) is noted for each analyte in orange. Control group (C), Low (L), Medium (M), High (H) and Extra High (Ex H).

		T0					T4					T10					T18				
Analyte	LOD (ng/L)	C	L	M	H	Ex H	C	L	M	H	Ex H	C	L	M	H	Ex H	C	L	M	H	Ex H
Benzothiophene	0.2	<LOD	<LOD	<LOD	<LOD	<LOD	<LOD	<LOD	<LOD	<LOD	<LOD	<LOD	<LOD	<LOD	<LOD	<LOD	<LOD	<LOD	<LOD	<LOD	<LOD
Napthalene	5.7	<LOD	<LOD	<LOD	97.3	388.3	<LOD	<LOD	<LOD	17.6	47.6	<LOD	<LOD	<LOD	6.6	16.0	<LOD	<LOD	<LOD	<LOD	<LOD
C1-NAP	11.8	<LOD	<LOD	200.5	1782.2	4126.9	<LOD	18.4	41.6	251.1	634.4	<LOD	16.5	25.8	107.7	273.7	<LOD	<LOD	18.8	97.8	39.0
C2-NAP	4.1	6.8	<LOD	140.4	1143.6	3210.4	<LOD	14.0	27.4	205.7	593.5	<LOD	11.9	20.1	79.1	206.3	<LOD	7.8	11.2	73.9	28.3
C3-NAP	4.5	17.2	24.0	287.4	2028.4	4105.4	8.7	24.4	43.7	540.4	1805.3	5.6	18.5	28.9	153.2	733.0	<LOD	12.4	19.1	233.3	46.0
C4-NAP	6.7	29.6	108.3	519.2	2058.8	3547.1	11.1	44.5	82.8	1044.7	2532.3	<LOD	30.7	48.4	457.6	1499.4	<LOD	21.0	35.9	851.8	164.3
Biphenyl	0.7	<LOD	<LOD	4.8	35.2	70.3	<LOD	<LOD	<LOD	6.6	10.5	<LOD	<LOD	<LOD	2.7	5.4	<LOD	<LOD	<LOD	1.8	<LOD
Acenaphthylene	0.4	<LOD	<LOD	1.6	15.5	29.8	<LOD	<LOD	<LOD	3.6	13.9	<LOD	<LOD	<LOD	1.1	5.3	<LOD	<LOD	<LOD	1.5	<LOD
Acenapthene	0.8	<LOD	<LOD	1.0	4.7	14.6	<LOD	<LOD	<LOD	<LOD	1.7	<LOD	<LOD	<LOD	<LOD	<LOD	<LOD	<LOD	<LOD	<LOD	<LOD
Dibenzofuran	0.8	<LOD	<LOD	6.6	32.8	62.3	<LOD	<LOD	1.4	6.3	10.0	<LOD	<LOD	1.1	3.2	5.1	<LOD	<LOD	<LOD	2.5	1.5
Fluorene	0.8	<LOD	0.9	7.6	37.6	86.1	<LOD	0.9	1.6	7.7	16.1	<LOD	0.9	1.3	3.3	6.5	<LOD	<LOD	<LOD	2.6	1.4
C1-FLU	1.1	2.1	11.6	40.8	220.6	493.3	1.4	4.3	6.2	47.2	182.2	<LOD	3.1	4.1	16.4	66.3	<LOD	2.0	2.4	25.1	5.3
C2-FLU	1.9	5.3	58.2	128.1	402.5	755.4	<LOD	12.2	18.8	168.3	544.5	<LOD	8.4	9.3	74.4	286.9	<LOD	5.7	6.6	173.9	30.1
C3-FLU	9.4	<LOD	32.5	46.0	107.5	196.4	<LOD	<LOD	<LOD	60.5	157.0	<LOD	<LOD	<LOD	37.7	87.0	<LOD	<LOD	<LOD	73.8	22.6
Phenathrene	3.4	<LOD	15.7	48.5	207.5	338.8	<LOD	4.9	8.5	40.4	124.2	<LOD	4.2	6.0	14.8	40.8	<LOD	<LOD	<LOD	10.9	4.6
Anthracene	0.7	<LOD	1.6	2.8	14.2	23.8	<LOD	<LOD	<LOD	7.2	15.6	<LOD	<LOD	<LOD	1.6	6.8	<LOD	<LOD	<LOD	5.3	<LOD
C1-PHE	1.2	4.5	54.5	125.7	543.4	853.6	1.8	11.4	18.1	196.3	570.4	1.5	8.3	9.9	63.0	284.5	1.6	5.1	6.4	103.0	15.0
C2-PHE	5.4	<LOD	47.5	101.1	261.7	300.0	<LOD	13.8	21.2	171.3	281.4	<LOD	10.0	12.8	110.3	222.3	<LOD	6.9	8.0	181.6	58.5
C3-PHE	3.6	<LOD	61.3	98.7	94.9	146.1	<LOD	15.8	20.2	69.7	175.4	<LOD	10.0	14.5	61.8	96.8	<LOD	5.9	8.4	103.0	55.8
C4-PHE	1.9	<LOD	47.7	74.9	36.9	87.4	<LOD	13.2	15.6	24.1	119.1	<LOD	7.9	15.0	21.1	41.6	<LOD	4.6	6.5	45.9	25.8
Dibenzothiophene	0.3	<LOD	1.9	6.6	29.0	57.1	<LOD	0.6	1.1	7.8	18.1	<LOD	0.4	0.7	3.6	8.5	<LOD	<LOD	0.3	6.2	1.3
C1-DBT	0.8	1.5	8.9	19.3	78.7	130.6	<LOD	2.3	3.2	27.8	83.0	<LOD	1.8	1.9	9.4	38.0	1.1	1.3	1.2	16.4	3.1
C2-DBT	0.7	<LOD	3.1	6.1	14.8	17.6	<LOD	1.1	1.4	10.0	16.1	<LOD	0.9	0.9	6.4	12.0	<LOD	<LOD	<LOD	10.7	4.2
C3-DBT	0.5	<LOD	3.2	4.8	4.7	7.4	<LOD	1.0	1.1	3.6	8.6	<LOD	0.7	0.8	3.1	4.8	<LOD	<LOD	<LOD	5.2	3.0
C4-DBT	0.4	<LOD	2.2	3.1	1.5	3.6	<LOD	0.7	0.8	1.0	4.7	<LOD	0.5	0.7	0.9	1.5	<LOD	<LOD	<LOD	1.8	1.0
Fluoranthene	0.9	1.6	1.4	2.1	6.3	8.2	1.6	<LOD	<LOD	3.3	6.2	1.5	<LOD	<LOD	1.9	3.9	2.0	<LOD	<LOD	2.6	<LOD
Pyrene	0.6	0.9	1.6	2.8	7.3	10.0	0.8	<LOD	0.8	4.2	8.6	0.7	0.7	<LOD	2.5	5.5	0.8	<LOD	<LOD	4.2	1.5
C1-FLA/PYR	0.8	1.4	13.7	26.7	49.6	81.9	1.4	9.8	5.3	29.5	101.8	<LOD	4.9	4.1	28.5	62.3	1.3	3.0	2.3	59.8	25.4
C2-FLA/PYR	0.2	0.2	7.3	15.4	11.5	25.9	<LOD	5.2	2.9	7.2	43.5	<LOD	2.7	2.9	8.0	16.9	<LOD	1.5	1.2	17.6	8.7
C3-FLA/PYR	0.3	<LOD	10.0	17.7	22.2	50.4	<LOD	6.3	3.6	11.5	61.9	<LOD	3.1	3.7	10.1	28.1	<LOD	1.8	1.9	22.4	8.3

Benz[a]anthracene	0.2	<LOD	0.4	0.5	0.8	1.4	<LOD	0.2	0.2	0.4	1.6	<LOD	<LOD	<LOD	0.5	0.7	<LOD	<LOD	<LOD	0.7	0.3
Chrysene	0.5	0.6	2.2	3.2	4.2	6.6	0.6	0.7	1.0	3.6	6.6	<LOD	0.6	0.6	2.6	4.1	<LOD	<LOD	0.6	4.0	2.1
C1-CHR	0.2	<LOD	4.4	6.7	4.0	9.2	<LOD	3.0	1.5	2.7	15.8	<LOD	1.4	1.4	3.1	5.8	<LOD	0.8	0.7	6.1	3.5
C2-CHR	0.1	<LOD	0.6	0.9	0.3	0.9	<LOD	0.4	0.2	0.2	1.9	<LOD	0.1	0.3	0.2	0.4	<LOD	<LOD	<LOD	0.4	0.2
C3-CHR	0.2	<LOD	0.5	0.8	0.2	0.9	0.2	<LOD	<LOD	<LOD	1.8	<LOD	<LOD	0.2	<LOD	0.3	<LOD	<LOD	<LOD	0.2	<LOD
C4-CHR	0.1	<LOD	0.5	0.9	0.2	0.9	<LOD	0.2	0.2	0.2	1.8	<LOD	0.2	0.3	<LOD	0.3	<LOD	<LOD	<LOD	0.3	<LOD
Benzo[b]fluoranthene	0.2	<LOD	0.4	0.5	0.2	0.6	<LOD	0.4	<LOD	<LOD	1.2	<LOD	0.4	<LOD	0.3	0.4	<LOD	0.2	<LOD	0.4	0.3
Benzo[k] fluoranthene	0.3	0.5	0.4	<LOD	<LOD	0.5	<LOD	0.4	<LOD	<LOD	0.8	0.3	<LOD	<LOD	<LOD	<LOD	<LOD	<LOD	<LOD	0.3	<LOD
Benzo[e]pyrene	0.2	0.2	0.5	0.6	0.3	0.6	0.2	0.4	0.2	0.2	1.3	<LOD	0.3	0.2	0.2	0.4	<LOD	<LOD	0.2	0.4	0.2
Benzo[a]pyrene	0.1	<LOD	0.2	0.2	0.2	0.3	0.1	0.2	<LOD	<LOD	0.3	<LOD	0.1	<LOD	<LOD	0.1	0.1	<LOD	<LOD	0.1	0.2
Perylene	0.02	<LOD	0.1	0.03	<LOD	0.1	<LOD	<LOD	<LOD	<LOD	0.1	<LOD	<LOD	0.05	<LOD	<LOD	<LOD	<LOD	<LOD	<LOD	<LOD
Idenol[1,2,3-cd]pyrene	0.1	<LOD	<LOD	<LOD	<LOD	<LOD	0.2	0.2	<LOD	<LOD	0.2	<LOD	0.2	<LOD	<LOD	<LOD	<LOD	<LOD	<LOD	<LOD	<LOD
Dibenz[ah]anthracene	0.1	<LOD	<LOD	<LOD	<LOD	<LOD	<LOD	0.1	<LOD	<LOD	0.2	<LOD	<LOD	<LOD	<LOD	<LOD	<LOD	<LOD	<LOD	<LOD	<LOD
Benzol[ghi]perylene	0.1	<LOD	0.1	0.2	<LOD	0.2	0.1	0.1	<LOD	<LOD	0.3	<LOD	0.1	<LOD	<LOD	<LOD	<LOD	<LOD	<LOD	<LOD	<LOD
Sum 44 PAH (ng/L)		**72.3**	**527.3**	**1954.9**	**9361.4**	**19250.9**	**28.1**	**211.0**	**330.5**	**2981.9**	**8221.7**	**9.7**	**149.5**	**216.0**	**1296.7**	**4077.7**	**7.0**	**80.0**	**131.7**	**2147.4**	**561.3**
Sum 44 PAH (µg/L)		**0.072**	**0.527**	**1.955**	**9.361**	**19.251**	**0.028**	**0.211**	**0.311**	**2.982**	**8.222**	**0.009**	**0.150**	**0.216**	**1.297**	**4.078**	**0.007**	**0.080**	**0.132**	**2.147**	**0.561**

In preparation data from Bender et al.

Bender ML, Giebichenstein J, Teisrud R, Laurent J, Frantzen M, Meador JP, Sørensen L, Hansen BH, Reinardy HC, Laurel B. Forthcoming 2020. Interactive effects of crude oil pollution and warming on polar cod early life stages.

All figures, descriptions and tables are exact copies from the unpublished data, including figure numbers. Only the figures and tables relevant to the data used in this thesis is added below.

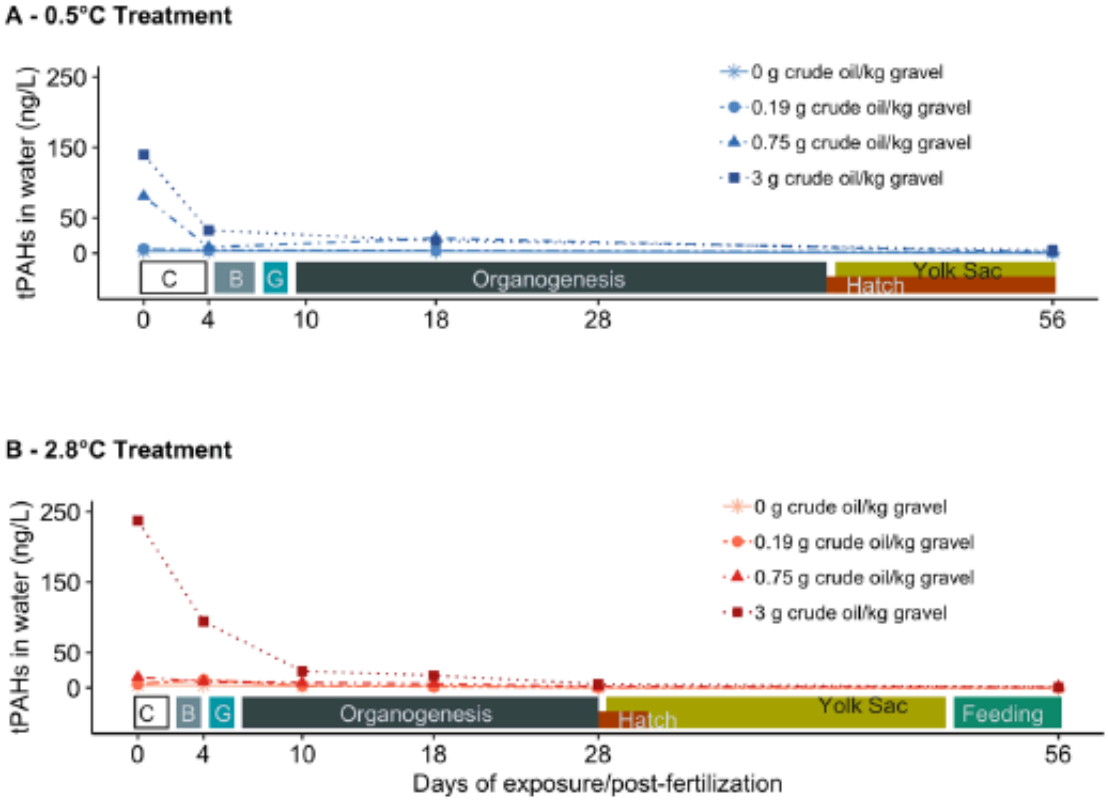

Figure 1. The concentration of tPAHs (ng/L) over time in the cooler, 0.5°C temperature group (top) and the warmer, 2.8°C temperature group (bottom). Different concentrations of crude oil and gravel are distinguished by color, shape and line type. The best linear model *lm(tPAH ~ Time + factor(Temperature) + factor(Oil Treatment)* reported the effects of time (F-value=6.09, p-value=0.019), temperature (F-value = 0.0211, p-value = 0.885) and oil treatment (F-value=4.5034, p-value=0.009). The developmental timeline of embryos and larvae in each temperature group are displayed in each panel. Early embryogenesis is divided into cleavage stage (C), blastulation (B), and gastrulation (G).

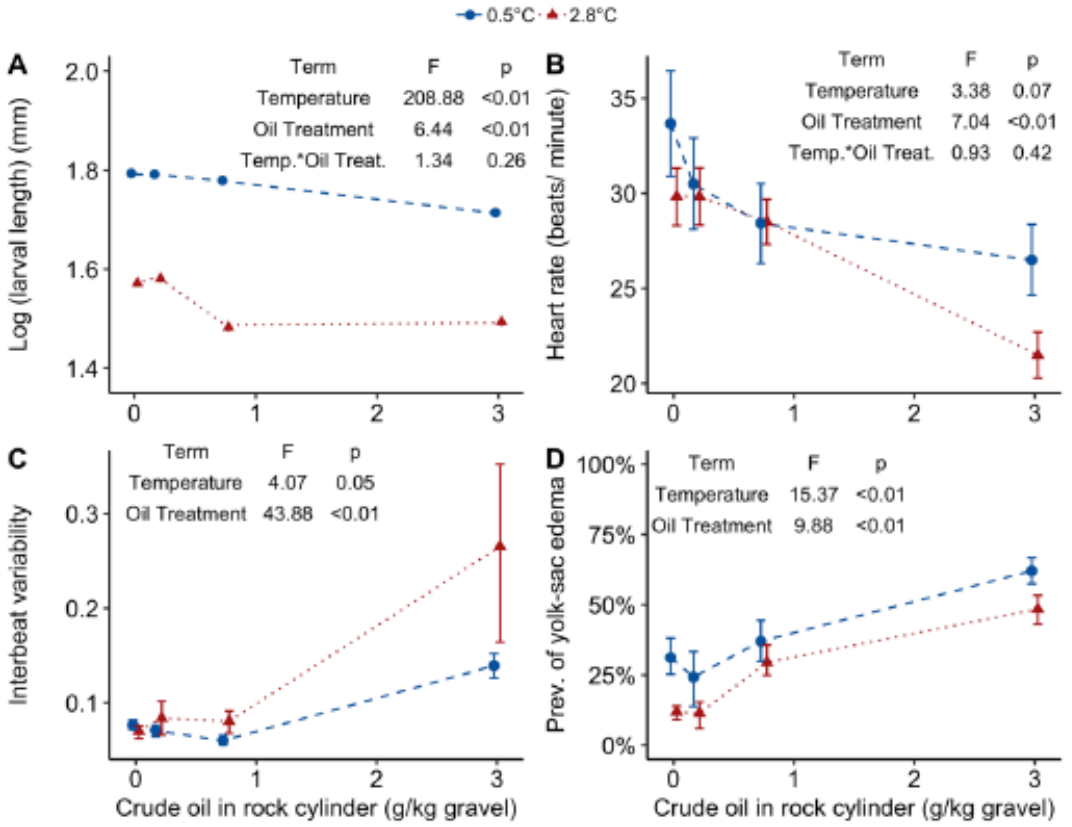

Figure 6. The effects of temperature and WSF crude oil exposure on yolk sac larvae: (A) log (length (mm)) at day 28 for 2.8°C and day 50 for 0.5°C displayed as incubator means (± SEM depicted as bars, each point includes 20-30 larvae); **(B) heart rate** and **(C) cardiac arrhythmia** at day 30-31 for 2.8°C and Day 48-49 for 0.5°C displayed as interbeat variability; and **(D) the prevalence of yolk sac edema** at day 28 for 2.8°C and day 50 for 0.5°C. Fitted dashed lines are the results of gls models using incubator as a random factor for panel A-C. For all panels, colors, line types, and shapes distinguish temperature groups and treatment means are plotted (± SEM depicted as bars, each point includes four incubator means calculated from 30 larvae (panel A) or three larvae each (panel B and C)). Panel D presents treatment means (± SEM depicted as bars, each point includes deformity scores (i.e. percentage of larvae afflicted) from four incubators) and the fitted line is a result of the lme model using incubator as a random factor. The terms of the best gls model for larval length, heart rate and arrhythmia and the best lme model for prevalence of yolk-sac edema are displayed in the respective panels with the ANOVA test F-values and p-values.

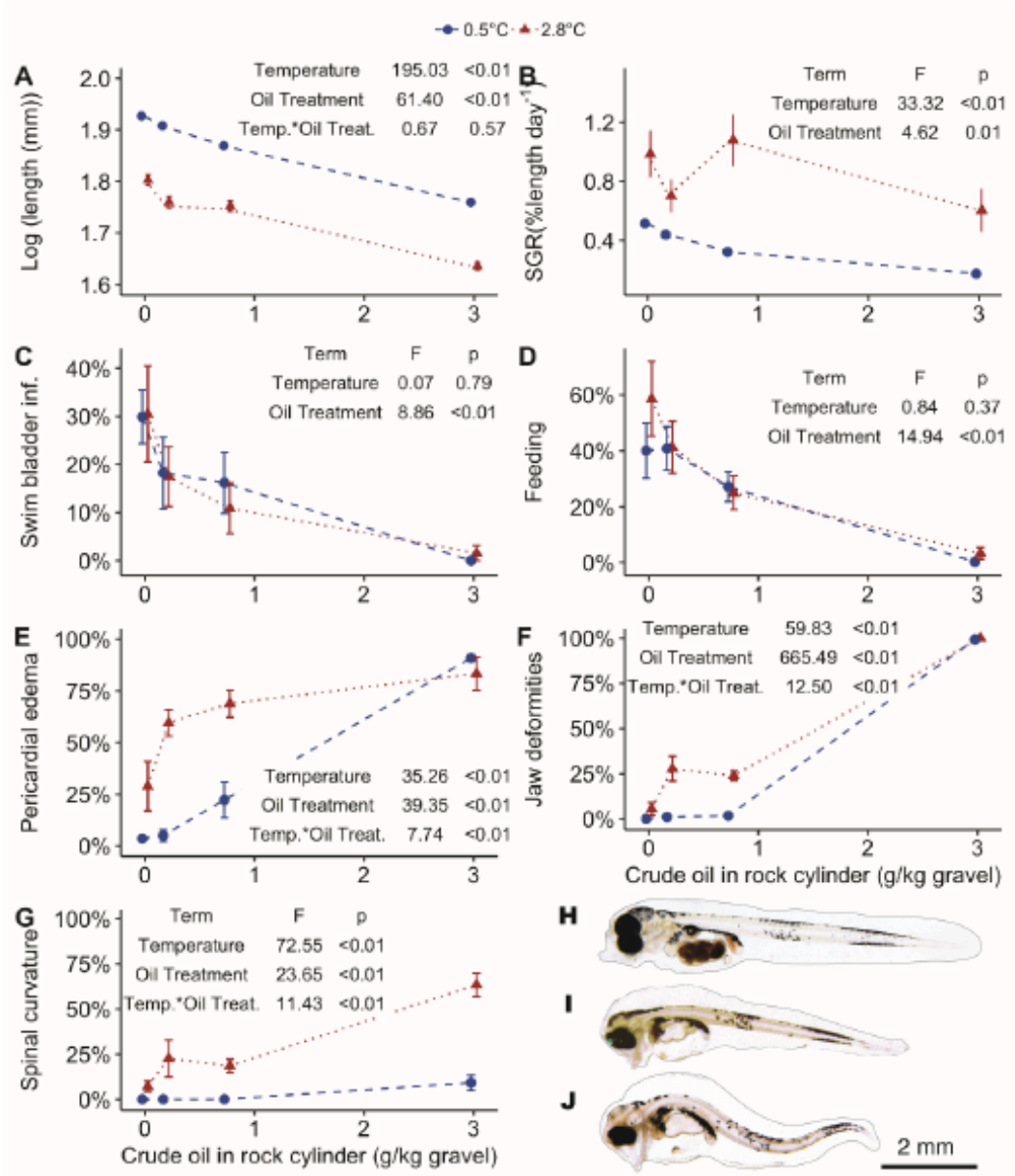

Figure 7. The effects of temperature and WSF crude oil exposure on exogenously feeding larvae (day 52 for 2.8°C and day 76 for 0.5°C) morphometrics, development and phenotype: **(A) log (length (mm))** of larvae represented as incubator means (± SEM depicted as bars, each point includes 30 larvae). **(B) The log of the specific growth rate (% length day^{-1})** displayed as CO treatment means (± SEM depicted as bars, each point includes four incubator means from 30 larvae). Fitted dashed lines are the result of a gls model using incubator as a random factor. The terms of the best gls model for larval length and SGR are displayed in the respective panels with the ANOVA test F-values and p-values. The prevalence of **(C) swim bladder inflation**; **(D) feeding**; **(E) pericardial edema**; **(F) jaw deformities**; and **(G) spinal curvature** is represented as treatment means (± SEM depicted as bars, each point includes 4 incubator deformity scores). Fitted dashed lines are the results of lme model using incubator as a random factor. The terms of the best lme models for each parameters is displayed in the respective panels with the associated ANOVA test F-values and p-values. For all panels, colors, shapes, and line types distinguish temperature groups. Typical phenotypes of exogenously feeding larva exposed to **(H) Control oil treatment in the cold group**; **(I) Cold, high oil treatment**; and **(J) warm, high oil treatment** are displayed in the lower right.

Table S2. Concentrations of the 44 PAH analytes measured in the water at the start of the exposure (Day 0) for each temperature and crude oil treatment group. Lower limit of detection (LOD) is noted for each analyte in the first column.

Analyte (ng/L)	LOD	0.5°C				2.8°C			
		Control	Low	Medium	High	Control	Low	Medium	High
Benzothiophene	0.07	0.10	0.13	0.18	0.21	0.14	0.10	0.12	0.15
Naphthalene	0.39	0.81	0.74	1.80	14.27	0.74	0.89	1.37	12.39
C1-NAP	0.05	0.10	0.27	1.90	16.84	0.09	0.53	1.34	16.47
C2-NAP	1.13	<LOD	<LOD	2.09	12.46	<LOD	<LOD	1.43	12.19
C3-NAP	0.02	0.05	0.41	6.04	20.10	0.06	0.53	1.52	31.62
C4-NAP	0.04	0.07	0.67	16.93	23.88	0.12	0.57	2.06	64.19
Biphenyl	0.13	0.24	0.26	0.68	4.00	0.21	0.40	0.67	3.16
Acenaphthylene	0.10	0.10	<LOD	0.40	1.25	0.11	0.13	0.23	1.98
Acenapthene	0.04	0.05	<LOD	0.17	0.57	0.05	<LOD	0.10	0.56
Dibenzofuran	0.15	0.19	0.21	0.61	2.87	0.20	0.29	0.49	2.41
Fluorene	0.12	0.14	0.20	0.73	3.78	0.15	0.28	0.54	3.06
C1-FLU	0.01	0.01	0.05	0.55	1.56	0.02	0.07	0.17	2.32
C2-FLU	0.01	0.02	0.14	3.36	3.28	0.03	0.10	0.34	9.85
C3-FLU	0.06	<LOD	0.07	2.27	1.08	<LOD	<LOD	0.13	5.20
Phenanthrene	0.14	0.24	0.72	4.54	14.22	0.82	0.84	1.89	15.41
Anthracene	0.88	<LOD	<LOD	0.97	<LOD	<LOD	<LOD	<LOD	2.71
C1-PHE	0.01	0.02	0.15	2.79	4.36	0.02	0.13	0.45	9.72
C2-PHE	0.25	<LOD	0.29	3.98	3.10	<LOD	0.26	0.59	6.48
C3-PHE	0.01	0.01	0.35	8.46	2.67	0.02	0.12	0.40	10.01
C4-PHE	0.12	<LOD	0.31	8.74	1.81	<LOD	<LOD	0.21	9.10
Dibenzothiophene	0.11	0.11	0.18	1.31	2.05	0.13	0.21	0.36	4.27
C1-DBT	1.76	<LOD	<LOD	<LOD	<LOD	<LOD	<LOD	<LOD	<LOD
C2-DBT	0.01	0.01	0.02	0.23	0.18	0.01	0.01	0.03	0.36
C3-DBT	0.01	<LOD	0.01	0.34	0.11	<LOD	0.01	0.02	0.40
C4-DBT	0.00	<LOD	0.01	0.25	0.06	0.00	0.00	0.01	0.26
Fluoranthene	0.22	0.23	0.35	0.79	0.76	0.25	<LOD	0.24	1.02
Pyrene	0.02	0.10	0.11	1.20	0.95	0.16	0.08	0.17	1.70
C1-FLA/PYR	0.01	0.01	0.10	1.50	1.08	0.02	0.04	0.16	2.18
C2-FLA/PYR	0.01	<LOD	0.07	1.06	0.44	<LOD	0.02	0.05	1.38
C3-FLA/PYR	0.01	<LOD	0.06	1.03	0.35	0.01	0.01	0.04	1.12
Benz[a]anthracene	0.06	<LOD	<LOD	0.78	0.11	<LOD	<LOD	<LOD	0.79
Chrysene	0.00	<LOD	0.05	2.67	0.92	<LOD	<LOD	0.07	2.76
C1-CHR	0.01	<LOD	0.04	0.61	0.19	<LOD	<LOD	0.03	0.70
C2-CHR	0.03	<LOD	<LOD	0.08	<LOD	<LOD	<LOD	<LOD	0.09
C3-CHR	0.01	<LOD	0.01	0.08	0.02	<LOD	0.02	<LOD	0.09
C4-CHR	0.02	<LOD	<LOD	0.07	<LOD	<LOD	<LOD	<LOD	0.08
Benzo[b]fluoranthene	0.03	<LOD	<LOD	0.35	0.11	<LOD	<LOD	<LOD	0.29
Benzo[k]fluoranthene	0.00	<LOD	<LOD	0.25	<LOD	<LOD	<LOD	<LOD	0.21
Benzo[e]pyrene	0.00	<LOD	<LOD	0.46	0.07	<LOD	<LOD	<LOD	0.37
Benzo[a]pyrene	0.00	<LOD	<LOD	0.28	<LOD	<LOD	<LOD	<LOD	<LOD
Perylene	0.00	<LOD	<LOD	0.12	<LOD	<LOD	<LOD	<LOD	0.06
Indeno[1,2,3-cd]pyrene	0.07	<LOD	<LOD	<LOD	<LOD	<LOD	<LOD	<LOD	<LOD
Dibenz[ah]anthracene	0.18	<LOD	<LOD	<LOD	<LOD	<LOD	<LOD	<LOD	<LOD
Benzo[ghi]perylene	0.00	<LOD	<LOD	0.11	<LOD	<LOD	<LOD	<LOD	0.11
Sum PAH		2.60	5.99	80.78	139.70	3.34	5.65	15.22	237.26
Sum NAP		1.03	2.10	28.76	87.55	1.01	2.52	7.72	136.86
Sum 2-3rings PAH		1.23	3.09	40.57	47.16	1.89	2.95	6.74	87.42
Sum 4-6rings PAH		0.34	0.81	11.45	4.99	0.44	0.17	0.76	12.98